


RESEARCH PAPER

A bivalent antihypertensive vaccine targeting L-type calcium channels and angiotensin AT₁ receptors

Hailang Wu^{1,2,3} | Yiyi Wang^{1,2,3} | Gongxin Wang⁴ | Zhihua Qiu^{1,2,3} | Xiajun Hu^{1,2,3} | Hongrong Zhang^{1,2,3} | Xiaole Yan^{1,2,3} | Fan Ke^{1,2,3} | Anruo Zou⁴ | Min Wang^{1,2,3} | Yuhua Liao^{1,2,3} | Xiao Chen^{1,2,3} 

¹Department of Cardiology, Union Hospital, Tongji Medical College, Huazhong University of Science and Technology, Wuhan, China

²Institute of Cardiology, Union Hospital, Tongji Medical College, Huazhong University of Science and Technology, Wuhan, China

³Key Lab for Biological Targeted Therapy of Education Ministry and Hubei Province, Union Hospital, Tongji Medical College, Huazhong University of Science and Technology, Wuhan, China

⁴Electrophysiological Laboratory, Qingdao Haiwei Biopharma Co. Ltd, Qingdao, China

Correspondence

Yuhua Liao and Xiao Chen, Department of Cardiology, Union Hospital, Tongji Medical College, Huazhong University of Science and Technology, Wuhan 430022, China.
Email: liaoyh27@163.com; skycreeper@126.com

Funding information

National Natural Science Foundation of China, Grant/Award Numbers: 81500388, 81600390 and 81670461; Major Research Plan of the National Natural Science Foundation of China, Grant/Award Number: 91439207; 7th "3551 China Optics Valley Talent Schema"

Background and Purpose: Hypertension has been the leading preventable cause of premature death worldwide. The aim of this study was to design a more efficient vaccine against novel targets for the treatment of hypertension.

Experimental Approach: The epitope CE12, derived from the human L-type calcium channel (Ca_v1.2), was designed and conjugated with Qβ bacteriophage virus-like particles to test the efficacy in hypertensive animals. Further, the hepatitis B core antigen (HBcAg)-CE12-CQ10 vaccine, a bivalent vaccine based on HBcAg virus-like particles and targeting both human angiotensin AT₁ receptors and Ca_v1.2 channels, was developed and evaluated in hypertensive rodents.

Key Results: The Qβ-CE12 vaccine effectively decreased the BP in hypertensive rodents. A monoclonal antibody against CE12 specifically bound to L-type calcium channels and inhibited channel activity. Injection with monoclonal antibody against CE12 effectively reduced the BP in angiotensin II-induced hypertensive mice. The HBcAg-CE12-CQ10 vaccine showed antihypertensive effects in hypertensive mice and relatively superior antihypertensive effects in spontaneously hypertensive rats and ameliorated L-NAME-induced renal injury. In addition, no obvious immune-mediated damage or electrophysiological adverse effects were detected.

Conclusion and Implications: Immunotherapy against both AT₁ receptors and Ca_v1.2 channels decreased the BP in hypertensive rodents effectively and provided protection against hypertensive target organ damage without obvious feedback activation of renin-angiotensin system or induction of dominant antibodies against the carrier protein. Thus, the HBcAg-CE12-CQ10 vaccine may provide a novel and promising therapeutic approach for hypertension.

Abbreviations: Ang II, angiotensin II; DHPs, 1,4-dihydropyridines; E3, the third extracellular region; HBcAg, hepatitis B core antigen; L-NAME, N^G-nitro-L-arginine methyl ester; mAb, monoclonal antibodies; MIR, major immunodominant region; RAS, renin-angiotensin system; SBP, systolic BP; SHRs, spontaneously hypertensive rats; TEM, transmission electron microscope; Tfh, follicular helper T cells; Th, T helper cells; VLP, virus-like particle

Hailang Wu and Yiyi Wang contributed equally to this work.

1 | INTRODUCTION

Hypertension has become the leading risk factor for death due to cardiovascular diseases and chronic kidney disease (Global Burden of Metabolic Risk Factors for Chronic Diseases Collaboration, 2014). The number of adults with hypertension increased dramatically in recent decades, with most of the increase occurring in developing countries (NCD Risk Factor Collaboration, 2017). Chemical drugs such as **angiotensin II** (Ang II) receptor blockers, **ACE** inhibitors, and calcium channel blockers are widely used in the treatment of hypertension and exhibit excellent therapeutic effects. Nevertheless, because treatment compliance is poor (Lobo, Sobotka, & Pathak, 2017), the control of BP is far from satisfactory (Mills et al., 2016). In comparison with chemical drugs, vaccines can elicit specific antibodies against hypertension-related target molecules and reduce dosing frequency, providing a possible solution to the current difficulties (Oparil & Schmieder, 2015). In a clinical trial, vaccination against Ang II (CYT006-AngQb) reduced mean ambulatory daytime BP from baseline by $-9/-4$ mmHg compared with placebo (Tissot et al., 2008). However, the antihypertensive effect of this vaccine cannot fully satisfy the clinical requirements (Whelton et al., 2018). In our view, this situation mainly results from three possible factors. First, the feedback activation of the renin-angiotensin system (RAS) induced by vaccination against Ang II may cripple the antihypertensive effect and target organ protection to some extent (Ambuhl et al., 2007; Fogari et al., 2011). Second, primary hypertension is basically a combined effect of several factors and combined medication therapy against different targets always achieves better prognosis (Mancia et al., 2013; Wald, Law, Morris, Bestwick, & Wald, 2009). Third, dominant antibodies against the carrier protein induced by the conjugated vaccine may have weakened the protective effect of vaccination (Dagan, Poolman, & Siegrist, 2010; Insel, 1995; Jegerlehner et al., 2010). Therefore, a novel vaccine that makes improvements in these aspects may provide several advantages.

Our previous study demonstrated that vaccination against **Ang II AT₁ receptors** decreased the systolic BP (SBP) in hypertensive animals and provided excellent protective effects in target organs without obvious feedback of the RAS (Chen et al., 2013; Zhu et al., 2006). To acquire sufficient antihypertensive effect, we are in urgent need of another target for the therapeutic vaccine (Mancia et al., 2013; Wald et al., 2009). The 1,4-dihydropyridines (DHPs) are widely used in the treatment of hypertension by inhibiting the voltage-gated **Ca_v1.2** calcium channel, the most prominent voltage-gated calcium channel type in vascular smooth muscle (Tang et al., 2016). The L-type voltage-gated calcium channel Ca_v1.2 consists of the pore-forming α_{1C} subunit and the auxiliary $\alpha_2\delta$ and β subunits and mediates Ca²⁺ entry into cells in response to membrane depolarization (Hofmann, Flockerzi, Kahl, & Wegener, 2014; Zamponi, Striessnig, Koschak, & Dolphin, 2015). Recent evidence indicated that the domains III and IV of the α_{1C} subunit play an important role in the allosteric modulation of Ca_v1.2 channels following DHP binding (Tang et al., 2016). Earlier work had discovered the importance of the third extracellular (E3) region for the function of ion channels (Xu et al., 2005).

What is already known

- Vaccine therapy can be advantageous in the treatment of hypertension and its complications.
- The antihypertensive effects of the CYT006-AngQb vaccine cannot fully satisfy clinical requirements.

What this study adds

- L-type calcium channels can be a novel therapeutic target for antihypertensive vaccine design.
- Antihypertensive vaccine against multiple targets may improve therapeutic efficacy.

What is the clinical significance

- The HBcAg-CE12-CQ10 vaccine may become a promising treatment for hypertension in humans.
- Construction strategy of the HBcAg-CE12-CQ10 vaccine may facilitate future antihypertensive vaccine design.

Hepatitis B core antigen (HBcAg) is structurally an icosahedral nucleocapsid and consists of 180 or 240 copies of identical hepatitis B core protein subunits (Roose, De Baets, Schepens, & Saelens, 2013). The major immunodominant region (MIR) of hepatitis B core protein (amino acids 76–82) is extremely immunogenic and exposed on the long protruding spikes of the HBcAg particle (Pumpens & Grens, 2001; Roose et al., 2013). The MIR successfully accommodated foreign sequences up to 238 amino acids in length and is considered the optimal target for the display of foreign epitopes and blockade of the epitopes of the carrier protein at the same time (Pumpens & Grens, 2001; Roose et al., 2013).

Here, a linear epitope CE12, derived from the E3 region of domain IV of the human Ca_v1.2 calcium channel α_{1C} subunit, was designed and tested for efficacy against hypertension. Furthermore, the CQ10 epitope (also called “the ATR-001 epitope”), derived from the second extracellular loop of human AT₁ receptors (Chen et al., 2013), and the CE12 epitope were both inserted into the MIR of the stabilized HBcAg virus-like particle (VLP; Lu, Chan, Ko, VanLang, & Swartz, 2015) to improve their immunogenicity (Bachmann & Jennings, 2010). The recombinant protein was designated as a novel bivalent vaccine, which was found to reduce SBP in hypertensive rodents effectively and was safe in general.

2 | METHODS

2.1 | Ethics, randomization, and blinding

All animal care and experimental procedures in the current study conformed to the Guide for the Care and Use of Laboratory Animals published by the United States National Institutes of Health and were

approved by the Institutional Authority for Laboratory Animal Care of China. All experiments in this study were conducted in a randomized manner. At the beginning of an animal experiment, animals were similar in age and weight. They were attributed to a group randomly according to the number generated by computer program. After assignment, the body weight was not significantly different. Data collection and evaluation of all experiments were performed without knowledge of the group identity.

2.2 | Peptide synthesis

The CQ10 peptide (also called “the ATR-001 peptide”), with the sequence C-A-F-H-Y-E-S-Q corresponding to an epitope of the second extracellular loop of human AT₁ receptors (Chen et al., 2013), and the CE12 peptide, with the sequence C-A-P-E-S-E-P-S-N-S-T-E corresponding to an epitope of the E3 region of domain IV of the human L-type calcium channel Ca_v1.2 α_{1C} subunit, were synthesized by GL Ltd (Shanghai, China). The purity was above 98% and was determined by HPLC and MS.

2.3 | Plasmid construction

The gene sequence encoding the human HBc antigen (UniProt accession no. P03147) with the C terminus truncated at amino acid 149 was used as a basic template for plasmid constructions and was further modified to accept the insertion of the coding sequence of foreign epitopes. First, both D29 and R127 residues of the polypeptide were replaced by cysteine residues to stabilize the VLP (Lu et al., 2015). Second, CE12 and CQ10 peptide sequences (arranged as CE12-CQ10-CE12-CQ10) were inserted between D78 and S81 and flanked by flexible linkers GGGGSGGGG. After codon optimization, the gene sequence coding for the fusion protein HBcAg-CE12-CQ10 was synthesized by Sangon Biotech (Shanghai, China) and introduced into the expression vector pET-28a(+) (Novagen Cat# 69864-3) by restriction sites *Nco* I and *Xho* I. The recombinant plasmid pET28-HBcAg-CE12-CQ10 was confirmed by sequencing.

2.4 | Vaccine preparation

The Q β -CQ10 vaccine (also called “the ATRQ β -001 vaccine”) and the Q β -CE12 vaccine were prepared as previously described (Chen et al., 2013). For HBcAg-CE12-CQ10 vaccine preparation, the recombinant plasmid was expressed in BL21 *Escherichia coli* (Thermo Fisher Scientific Cat# C600003). After sonication of the cells, the fusion protein expressed as inclusion bodies was centrifuged (4 °C, 15 min, 12 000 x g). The pellet was washed by inclusion body washing buffer (50 mmol·L⁻¹ of Tris-Cl, pH 8.0; 0.2% Triton-X 100) and centrifuged again (4 °C, 15 min, 12 000 x g). Thereafter, the pellets were suspended in 50 mmol·L⁻¹ of Tris-Cl containing 2 mol·L⁻¹ of urea, stirred for 30 min and then centrifuged (4 °C, 15 min, 12 000 x g). After being washed repeatedly, the inclusion body pellets were suspended in inclusion body dissolving buffer (50 mmol·L⁻¹ of Tris-Cl, pH 8.0; 8 mol·L⁻¹ of urea) and stirred for at least 4 hr and then

centrifuged (4 °C, 15 min, 12 000 x g). Mercaptoethanol (final concentration, 5 mmol·L⁻¹) GSH (0.5 mmol·L⁻¹), and GSSG (0.1 mmol·L⁻¹) were added to the supernatant and dialysed against renaturation buffer (Tris-Cl (50 mmol·L⁻¹), GSH (0.5 mmol·L⁻¹), GSSG (0.1 mmol·L⁻¹); pH 8.0) containing 8 mol·L⁻¹ of urea with vigorous stirring. The dialysis outer solution was mixed with renaturation buffer at a constant flowrate of 0.5 ml·min⁻¹ until the urea concentration decreased to 1 mol·L⁻¹. After dialysis against 10 mmol·L⁻¹ of PBS (NaCl, 137 mmol·L⁻¹; KCl, 2.7 mmol·L⁻¹; Na₂HPO₄, 4.3 mmol·L⁻¹ and KH₂PO₄, 1.4 mmol·L⁻¹; pH 7.4) for 12 hr, the inner solution was loaded onto a Sepharose CL-4B column for gel filtration chromatography. The fractions were collected and identified by SDS-PAGE and transmission electron microscope (TEM). Antibody (Abcam Cat# ab8639, RRID:AB_306686) against HBcAg was used to test the exposure of the carrier protein. The vaccine concentration was determined using Bradford protein assay kit (Thermo Fisher Scientific Cat# 23200).

2.5 | Antibody preparation

Male BALB/c mice (MGI Cat# 2161059, RRID:MGI:2161059) aged 8 weeks (weight of 20–22 g) were immunized with Q β -CE12 vaccine at intervals of 2 weeks. According to the ELISA results, the splenocytes from the mice which showed the highest anti-CE12 titre were harvested and fused with Sp2/0 myeloma cells (ATCC Cat# CRL-1581, RRID:CVCL_2199, ATCC, Manassas, VA, USA) by the PEG method (Karpas, Dremucheva, & Czepulkowski, 2001). The hybridoma cell clone which stably secreted monoclonal antibodies (mAb) against CE12 was cultured and injected intraperitoneally into the pristane pretreated mice. Ascites fluid was harvested and initially purified using protein A affinity chromatography (Bio-Rad, Hercules, CA, USA). The final mAb-CE12 was obtained by a second purification using epitope-linked gel affinity chromatography (GE Healthcare, Piscataway, NJ, USA). The final working concentration of the antibody was 1.0 μ g·ml⁻¹, unless otherwise indicated. The antibody titres were determined by ELISA. The peptide neutralization antibody was produced by the co-incubation of 1 mg of CE12 peptide and 1 mg of the mAb-CE12 in PBS for 8 hr at 4°C. The monoclonal antibody against CQ10 was prepared accordingly. Normal mouse IgG (Santa Cruz Biotechnology Cat# sc-2025, RRID:AB_737182) was used as control antibody.

2.6 | Animals

Animal studies are reported in compliance with the ARRIVE guidelines (Kilkenny, Browne, Cuthill, Emerson, Altman, & Group, 2010; McGrath & Lilley, 2015) and with the recommendations made by the *British Journal of Pharmacology*. Male BALB/c mice aged 6 weeks (weight of 18–22 g) and male spontaneously hypertensive rats (SHRs, RGD Cat# 61000, RRID:RGD_61000) aged 3 weeks (weight of 35–45 g) were purchased from Vital River Laboratories in China (Beijing). The SHR model is a cornerstone of medical research in experimental hypertension and widely used for the screening of antihypertensive agents (Leong, Ng, & Jaarin, 2015). In addition, Ang II-induced

hypertension is another commonly employed model of hypertension (Leong et al., 2015). All animals were kept in stainless polypropylene cages with wood shavings as bedding materials under a constant 12-hr light-dark cycle at a controlled temperature (21–23°C) in the specific-pathogen-free room in the Animal Center of Tongji Medical College of Huazhong University of Science and Technology. Standard water and chow were provided ad libitum. At the end of the experiment, animals were killed by cervical vertebra dislocation.

Experiment 1: Four-week-old male SHR (n = 8 per group, two rats per cage) were immunized subcutaneously on Days 0, 14, 28, and 56 with Q β -CE12 vaccine or Q β VLP formulated in aluminum hydroxide gel (InvivoGen Cat# vac-alu-250), 400 μ g per rat. The control group was injected subcutaneously with the same volume of PBS. Another group was treated with peroral **amlodipine** (5 mg·kg⁻¹·day⁻¹; Pfizer) from Day 35. Anti-CE12-specific antibody titres were detected on Days 7, 21, 35, and 63. SBP was measured on Days 0, 8, 15, 22, 30, 37, 43, 50, and 65.

Experiment 2: Seven-week-old male BALB/c mice (n = 8 per group, four mice per cage) were injected with 50 μ g of mAb-CE12 or 100 μ g of mAb-CE12 via the tail vein once a week. Another group was injected 50 μ g of normal mouse IgG (Santa Cruz Biotechnology Cat# sc-2025, RRID:AB_737182). The control group received the same volume of PBS. All the mice were anaesthetized with 2% (v/v) isoflurane; then an osmotic minipump (model 2002, Alzet, Cupertino, CA, USA) filled with Ang II (1.4 mg·kg⁻¹·day⁻¹, Sigma-Aldrich Cat# A9525) was implanted subcutaneously under aseptic conditions on Day 7 to deliver Ang II for 14 days. Anti-CE12-specific antibody titres and SBP were detected on Days 3, 10, 15, and 23.

Experiment 3: Seven-week-old male BALB/c mice were randomly divided into four groups (n = 8 per group, four mice per cage). Animals in the vaccine group were immunized subcutaneously on Days 0, 14, and 28 with 200 μ g of Q β -CE12 vaccine formulated in aluminum hydroxide gel. Another group of mice was treated with peroral amlodipine (5 mg·kg⁻¹·day⁻¹; Pfizer) from Day 14. Animals in the last two groups were injected with the same volume of PBS. Except for the control group, all the mice were anaesthetized on Day 15, and an osmotic minipump (model 2002, Alzet) filled with Ang II (1.4 mg·kg⁻¹·day⁻¹, Sigma-Aldrich Cat# A9525) was implanted subcutaneously under aseptic conditions to deliver Ang II for 14 days. Anti-CE12-specific antibody titres were detected on Days 3, 10, 17, 24, and 31. SBP was measured on Days 4, 11, 22, and 29.

Experiment 4: Four-week-old male SHR were divided into six groups (n = 8 per group, two rats per cage). The vaccine groups were immunized subcutaneously on Days 0, 14, 28, 56, 84, and 98 with 400 μ g of Q β -CQ10, Q β -CE12 or HBcAg-CE12-CQ10 vaccine formulated in aluminum hydroxide gel, respectively. Another group was treated with peroral amlodipine (5 mg·kg⁻¹·day⁻¹; Pfizer) and **valsartan** (3 mg·kg⁻¹·day⁻¹; Novartis) from Day 14. The last two groups received the same volume of PBS accordingly. To induce renal injury, SHR not in the control group were administered the NOS inhibitor, L-NAME (185.4 μ mol·L⁻¹; Sigma-Aldrich Cat# N5751) in drinking water from Day 84 to Day 112 (Leong et al., 2015). Anti-CE12-specific antibody and anti-CQ10-specific antibody titres were detected on Days 3, 17,

32, 48, 60, 74, 88, 102, and 116. SBP was measured on Days 2, 16, 31, 46, 60, 73, 86, 100, and 114. The SHR were killed by cervical vertebra dislocation at 22 weeks of age. The heart, kidney, lung, and liver in each rat were immediately excised for later assessments.

Experiment 5: Seven-week-old male BALB/c mice were randomly divided into four groups (n = 8 per group, four mice per cage). Mice in the vaccine group were immunized subcutaneously on Days 0, 14, and 28 with 200 μ g of HBcAg-CE12-CQ10 vaccine formulated in aluminum hydroxide gel. Another group was treated with peroral amlodipine (5 mg·kg⁻¹·day⁻¹; Pfizer) and valsartan (3 mg·kg⁻¹·day⁻¹; Novartis) from Day 14. Mice in the last two groups received the same volume of PBS. Except for the control group, all the mice were anaesthetized on Day 15, and an osmotic minipump (model 2002, Alzet) filled with Ang II (1.4 mg·kg⁻¹·day⁻¹, Sigma-Aldrich Cat# A9525) was implanted to deliver Ang II for 14 days. Anti-CE12-specific antibody and anti-CQ10-specific antibody titres were detected on Days 3, 10, 17, 24, and 31. SBP was measured on Days 4, 11, 22, and 29.

Experiment 6: BALB/c mice are widely used in immunological studies (Ngiow, Loi, Thomas, & Smyth, 2016). To study the immune responses of HBcAg-CE12-CQ10 vaccination, 7-week-old male BALB/c mice were divided into three groups (n = 6 per group, four to five mice per cage). All mice in three groups were immunized subcutaneously with 200 μ g of HBcAg-CE12-CQ10 vaccine on Day 0, and two groups of mice were killed on Day 0 or Day 7, respectively. Mice in the third group were immunized subcutaneously with 200 μ g of HBcAg-CE12-CQ10 vaccine on Day 14 and killed by cervical vertebra dislocation on Day 21. The spleen and serum of each mouse were collected for further assessments.

2.7 | BP measurement

It was considered that the non-invasive tail-cuff method is more suitable for measuring BP for long-term observations (Leong et al., 2015). Therefore, the BP of animals was measured using the conventional tail-cuff method according to the manufacturer's instructions (BP-98a, Softron, Japan). All animals were trained for 1 week before the measurement. Animals were placed in a dark chamber at 37°C for 15 min and then transferred to a dark cage with a heating pad. The tail-cuff pressure was continuously monitored, and the signals from the pulse and pressure sensors were recorded. The SBP was calculated from six readings for each animal. All the measurements were performed by one person who was blinded to the identities of the groups in a quiet environment at 21–23°C between 9 and 11 a.m.

2.8 | ELISA

Serially diluted serum samples were added to 96-well plates pre-coated with CE12 peptide, CQ10 peptide, or HBcAg and incubated at 37°C for 2 hr. After five washes with PBS-Tween 20 (0.05%, v/v) solution, the plate was covered with Biotin-labelled antibody and incubated for 1 hr at 37°C. HRP-labelled streptavidin was added to bind with biotin-labelled antibody for another 1 hr, and 3,3',5,5'-tetramethylbenzidine

chromogenic solution was used to react with HRP for colour reaction. The absorbance of each well was determined at 450 nm using a microplate reader (Elx800, Bio-Tek, VT, USA). The antibody titre was calculated as the reciprocal of half maximum dilution with an absorbance greater than 0.1 and twofold higher than control at the same dilution. Antibody titres were occasionally logarithmically transformed to present the data on different orders of magnitude.

2.9 | Echocardiography

Animals were anaesthetized with 2% isoflurane and kept warm on a heating platform, and echocardiography was performed with a Vevo 2100 high-resolution microimaging system (Vevo 2100, RRID:SCR_015816, VisualSonics, Canada). Both long-axis and short-axis views of the left ventricle were obtained. Left ventricular end-diastolic dimension, left ventricular end-systolic dimension, left atrial end-systolic dimension, left atrial end-diastolic dimension, interventricular septal diastolic/systolic thickness, left ventricular posterior wall diastolic/systolic thickness, left ventricular anterior wall diastolic/systolic thickness, left ventricular ejection fraction, and fractional shortening were measured.

2.10 | Biochemical measurement

The plasma samples were used for the measurement of creatinine and blood urea nitrogen. Urine samples were collected using metabolic cages, and the supernatant was used for examination of the 24-hr urinary protein.

2.11 | Histopathology

Animals were killed at the end of the study, and the heart, liver, lung, and kidney were rapidly excised as soon as the animal was killed. Parts of fresh left renal cortex were immediately fixed in 0.25% glutaraldehyde for TEM. The tissue and organs were routinely fixed in 4% paraformaldehyde overnight, embedded in paraffin for histopathology. Sections were stained with haematoxylin–eosin or Masson's trichrome. Quantitative analysis of the pathological changes was conducted by Image-Pro Plus v6.0 (Image-Pro Plus, RRID:SCR_007369).

2.12 | Antibody identification

Immunofluorescence was used to demonstrate that the mAb-CE12 specifically bound to voltage-dependent L-type $Ca_v1.2$ calcium channel α_{1C} subunit. HEK293 cells (ATCC Cat# CRL-1573, RRID:CVCL_0045, ATCC) were stably transfected with a pcDNA3.1 (+) vector (Thermo Fisher Scientific Cat# V79020) expressing FLAG tagged-human $Ca_v1.2$ calcium channel α_{1C} subunit which was constructed by our lab and cultured in DMEM containing 10% FBS. The cells were fixed with 4% paraformaldehyde at -20°C for 5 min and co-incubated with mAb-CE12 and monoclonal anti-FLAG antibody (Sigma-Aldrich Cat# F1804, RRID:AB_262044, M2, 1:2000) overnight at 4°C . An Alexa

488 Fluor-conjugated antibody (Thermo Fisher Scientific Cat# A32723, RRID:AB_2633275, 1:200) was used as the secondary antibody. The preparation was imaged using an Olympus FV500 confocal microscope (Japan).

2.13 | Electrophysiology

Whole-cell calcium currents were recorded in HEK293 cells stably expressing L-type calcium channel $Ca_v1.2$ using the whole-cell patch-clamp configuration. Cells were perfused with a solution containing $BaCl_2$ ($20\text{ mmol}\cdot\text{L}^{-1}$), HEPES ($10\text{ mmol}\cdot\text{L}^{-1}$), glucose ($5\text{ mmol}\cdot\text{L}^{-1}$), $MgCl_2$ ($1\text{ mmol}\cdot\text{L}^{-1}$) and choline chloride ($1\text{ mmol}\cdot\text{L}^{-1}$), adjusted to pH 7.4. Patch electrodes were filled with a solution containing CsCl ($130\text{ mmol}\cdot\text{L}^{-1}$), HEPES ($10\text{ mmol}\cdot\text{L}^{-1}$), Na_2ATP ($3\text{ mmol}\cdot\text{L}^{-1}$), Na_2GTP ($0.1\text{ mmol}\cdot\text{L}^{-1}$), $MgCl_2$ ($1.5\text{ mmol}\cdot\text{L}^{-1}$), glucose ($10\text{ mmol}\cdot\text{L}^{-1}$), EGTA ($10\text{ mmol}\cdot\text{L}^{-1}$), and $MgATP$ ($0.5\text{ mmol}\cdot\text{L}^{-1}$) and adjusted to pH 7.3. $BaCl_2$ was used as a charge carrier to guarantee stable currents. To elicit inward Ca^{2+} currents, the -60 to $+40$ mV was applied in 10-mV increments. After obtaining whole-cell currents, nifedipine ($0.1\text{ }\mu\text{mol}\cdot\text{L}^{-1}$) was used to verify the identity of the Ca^{2+} currents.

HEK293 cells stably expressing hERG potassium channels ($K_v11.x$) were used for hERG current recordings. The extracellular solution contained NaCl ($137\text{ mmol}\cdot\text{L}^{-1}$), KCl ($4\text{ mmol}\cdot\text{L}^{-1}$), $CaCl_2$ ($1.8\text{ mmol}\cdot\text{L}^{-1}$), $MgCl_2$ ($1\text{ mmol}\cdot\text{L}^{-1}$), glucose ($10\text{ mmol}\cdot\text{L}^{-1}$), and HEPES ($10\text{ mmol}\cdot\text{L}^{-1}$), pH 7.4. Patch electrodes were filled with a solution containing KCl ($130\text{ mmol}\cdot\text{L}^{-1}$), $MgCl_2$ ($1\text{ mmol}\cdot\text{L}^{-1}$), EGTA ($5\text{ mmol}\cdot\text{L}^{-1}$), $MgATP$ ($5\text{ mmol}\cdot\text{L}^{-1}$) and HEPES ($10\text{ mmol}\cdot\text{L}^{-1}$), pH 7.2.

HEK293 cells stably expressing $Na_v1.5$ sodium channels were used for $Na_v1.5$ current recordings. The patch electrodes were filled with a solution containing NaCl ($20\text{ mmol}\cdot\text{L}^{-1}$), CsCl ($130\text{ mmol}\cdot\text{L}^{-1}$), EGTA ($10\text{ mmol}\cdot\text{L}^{-1}$) and HEPES ($10\text{ mmol}\cdot\text{L}^{-1}$), with pH adjusted to 7.2 with CsOH. The bath solution contained NaCl ($70\text{ mmol}\cdot\text{L}^{-1}$), CsCl, ($80\text{ mmol}\cdot\text{L}^{-1}$), KCl, ($5.4\text{ mmol}\cdot\text{L}^{-1}$), $CaCl_2$, ($2\text{ mmol}\cdot\text{L}^{-1}$), HEPES ($10\text{ mmol}\cdot\text{L}^{-1}$), glucose ($10\text{ mmol}\cdot\text{L}^{-1}$), and $MgCl_2$ ($1\text{ mmol}\cdot\text{L}^{-1}$), with pH adjusted to 7.4 with CsOH. The currents were amplified using a Digital 1550A (Axon Instruments, Silicon Valley, CA, USA) and analysed using Clampex software 10.6 (AXON, CA, USA). The steady-state activation curve was fitted to the Boltzmann equation: $G/G_{max} = a/[1 + \exp[-(V - V_{1/2})/k]]$, where G is the conductance, V is the test potential, $V_{1/2}$ represents the point where channels are half-activated, and k is the slope factor. The inactivation curve was fitted to the Boltzmann equation: $(I - I_0)/(I_{max} - I_0) = a/[1 + \exp(V - V_{1/2})/k]$, where I_{max} represents the current measured at the most hyperpolarized preconditioning pulse, I_0 represents a non-inactivating current at the most depolarized preconditioning pulse, and $V_{1/2}$ represents the point where channels are half-inactivated.

2.14 | Flow cytometry

The spleen from each BALB/c mouse was separated and grinded to cell suspension. Density gradient centrifugation was used to isolate mononuclear cells. The cells were stimulated with T cell activation

stimulator cocktail (with Brefeldin A; BioLegend Cat# 423303, San Diego, CA, USA) for 4 hr and washed with PBS and then incubated with anti-mouse CD4-FITC antibody (BD Biosciences Cat# 553650, RRID:AB_394970; BD Biosciences, San Jose, CA, USA) on ice for 30 min, washed twice in Perm/Wash Buffer (BD Biosciences Cat# 553650), and stained with anti-mouse IFN- γ PE-Cy7 (BD Biosciences Cat# 561040, RRID:AB_2034014), anti-mouse IL-4-PE (BD Biosciences Cat# 554435, RRID:AB_395391), anti-mouse IL-17-PE (BD Biosciences Cat# 559502, RRID:AB_397256), or anti-mouse CXCR5-PE (BD Biosciences Cat# 561988, RRID:AB_10893355) and anti-mouse CD279-APC (BD Biosciences Cat# 561988, RRID:AB_10893355) antibodies on ice for 30 min. BD LSRII flow cytometer system (BD Biosciences) was used to test the cell samples. The data were collected by FACSDiva v8.0.1 (BD FACSDiva Software, RRID:SCR_001456; BD Biosciences) and FlowJo software v10 (FlowJo, RRID:SCR_008520; FlowJo LLC, Ashland, OR, USA).

2.15 | Data and statistical analysis

The data and statistical analysis comply with the recommendations on experimental design and analysis in pharmacology (Curtis et al., 2018). Studies were designed to generate groups of equal size using randomization and blinded analysis. In the study of antihypertensive effects of vaccines, the group sizes were selected to detect a 10-mmHg reduction of SBP, assuming an *SD* of 6 mmHg, with a power of 80%. In the patch-clamp experiments, group sizes were selected on the basis of a previous study indicating that $n = 6$ per group may provide sufficient power for detecting the activities of L-type calcium channel (Liao et al., 2016). In the immunological studies, group sizes were selected on the basis of another study indicating that $n = 6$ may be sufficient for study of immune responses induced by vaccination (Hu et al., 2017). All the group sizes indicate the number of independent values, and the statistical analysis used these independent values.

Data are shown as mean \pm SEM. Statistical analysis was undertaken only for studies where each group size was at least $n = 5$. No data points were excluded from statistical analysis in any experiment. Two-way repeated measures ANOVA was used to analyse the data of BP and heart rates. Two-way ANOVA was used to analyse I-V curve, activation curve, and inactivation curve. One-way ANOVA was used to analyse pathological data and biochemical data among groups. Tukey's post hoc tests were conducted only if the *F* statistic was significant and there was no significant variance inhomogeneity. Survival rate was estimated using the Kaplan-Meier product limit method, and differences among the groups were assessed by the log-rank (Mantel-Cox) test. In all cases, $P < .05$ was considered statistically significant. Statistical analysis was performed using GraphPad Prism 5.0 (GraphPad Prism, RRID:SCR_002798, La Jolla, CA, USA).

2.16 | Materials

DMEM (Thermo Fisher Scientific Cat# 41965062), FBS (Thermo Fisher Scientific Cat# 10099141), BL21 *E. coli* (Thermo Fisher

Scientific Cat# C600003), Bradford protein assay kit (Thermo Fisher Scientific Cat# 23200), and pcDNA3.1 (+) vector (Thermo Fisher Scientific Cat# V79020) were purchased from Thermo Fisher Scientific Inc. (MA, USA). The CQ10 peptide and the CE12 peptide were synthesized by GL Ltd. The plasmid pET-28a(+) (Novagen Cat# 69864-3) was purchased from Novagen (Madison, WI, USA). Antibody against HBcAg (Abcam Cat# ab8639, RRID:AB_306686) was purchased from Abcam (Cambridge, UK). Normal mouse IgG (Santa Cruz Biotechnology Cat# sc-2025, RRID:AB_737182) was purchased from Santa Cruz Biotechnology (Dallas, TX, USA). Aluminum hydroxide gel (InvivoGen Cat# vac-alu-250) was purchased from InvivoGen (San Diego, CA, USA). Osmotic minipumps (model 2002, Alzet) were purchased from Alzet. Ang II (Sigma-Aldrich Cat# A9525) and L-NAME (Sigma-Aldrich Cat# N5751) were purchased from Sigma-Aldrich, Inc. (St. Louis, MO, USA). Antibodies against mouse CD4 (BD Biosciences Cat# 553650, RRID:AB_394970), IFN- γ (BD Biosciences Cat# 561040, RRID:AB_2034014), IL-4 (BD Biosciences Cat# 554435, RRID:AB_395391), IL-17 (BD Biosciences Cat# 559502, RRID:AB_397256), CXCR5 (BD Biosciences Cat# 561988, RRID:AB_10893355), and CD279 (BD Biosciences Cat# 561988, RRID:AB_10893355) were purchased from BD Biosciences.

2.17 | Nomenclature of targets and ligands

Key protein targets and ligands in this article are hyperlinked to corresponding entries in <http://www.guidetopharmacology.org>, the common portal for data from the IUPHAR/BPS Guide to PHARMACOLOGY (Harding et al., 2018), and are permanently archived in the Concise Guide to PHARMACOLOGY 2017/2018 (Alexander, Christopoulos et al., 2017; Alexander, Fabbro et al., 2017a, 2017b; Alexander, Striessnig et al., 2017).

3 | RESULTS

3.1 | CE12 vaccination effectively decreases BP of hypertensive rodents

After acclimatization, male SHR aged 4 weeks were immunized subcutaneously on Days 0, 14, 28, and 56 with Q β -CE12 or Q β VLP (Figure 1a). Anti-CE12-specific antibody was successfully elicited in SHR after Q β -CE12 vaccination. The antibody titre in the vaccine group rose on Day 7 after the first vaccination, peaked on Day 35, and declined thereafter (Figure 1b). Accordingly, SBP levels of SHR immunized with the Q β -CE12 vaccine were decreased compared with the VLP group, with a maximum decrease of 13 mmHg (199 ± 4 vs. 212 ± 3 mmHg, Figure 1c). The maximum SBP decrease was slightly less than that after amlodipine. No significant differences in SBP were found between the control group and the VLP group. The heart rates of the SHR showed no difference (Figure 1d). In another study, male BALB/c mice aged 7 weeks were injected with monoclonal antibody against CE12 (mAb-CE12) via the tail vein to study the antihypertensive effect (Figure 1e). In mAb-CE12-injected BALB/c mice, anti-

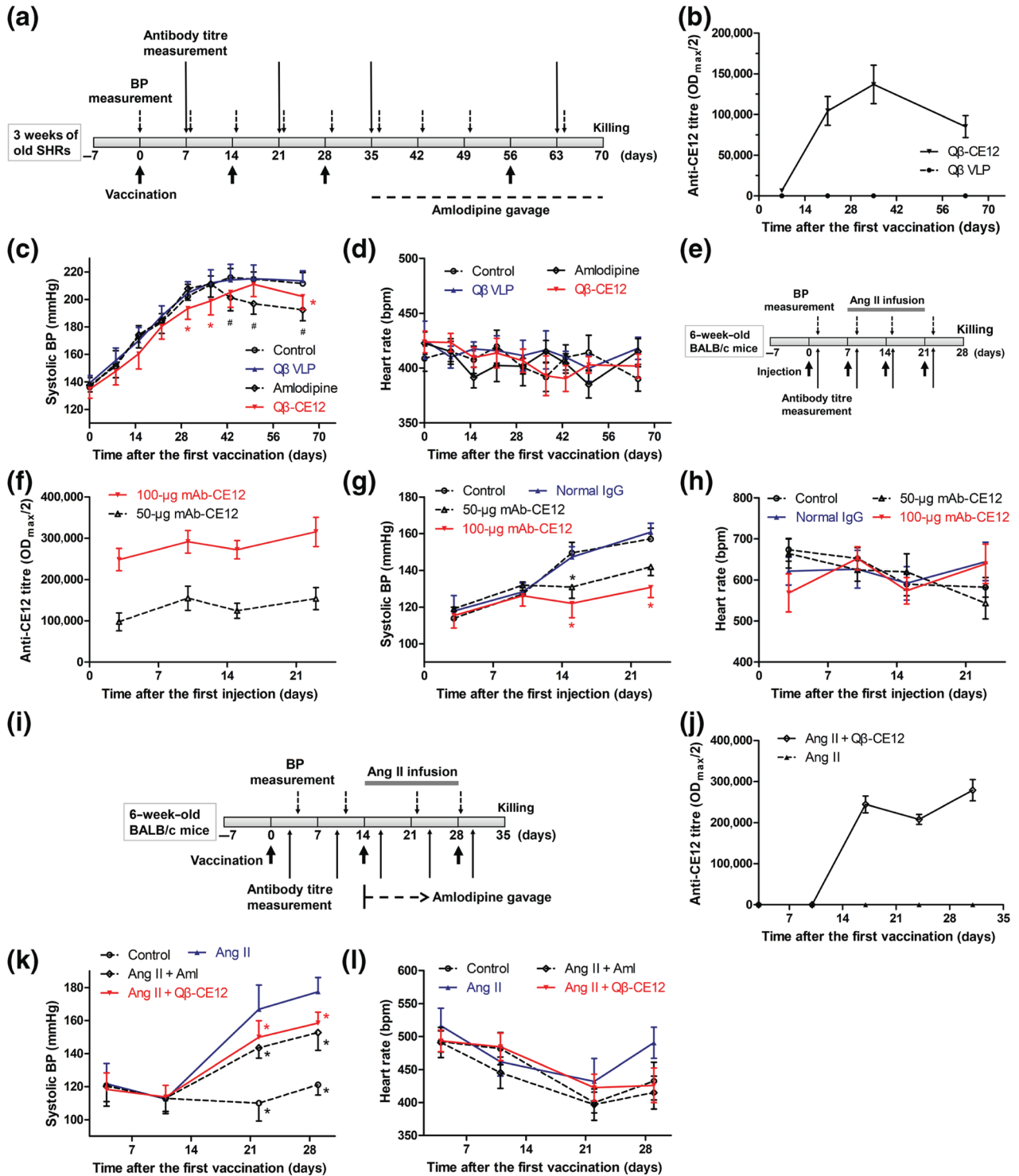


FIGURE 1 Q β -CE12 vaccination effectively decreases BP in hypertensive rodents. (a) Schematic timeline for the study of effects of Q β -CE12 vaccination in spontaneously hypertensive rats (SHRs). (b) Anti-CE12-specific antibody in response to Q β -CE12 vaccination in Q β -CE12 or Q β VLP immunized SHRs (ELISA on serum samples, $n = 8$ per group). (c) Systolic BP in response to Q β -CE12 vaccination in SHRs ($n = 8$ per group). * $P < .05$ significantly different from the VLP group, # $P < .05$, significantly different from the control group. (d) Heart rate of the SHRs ($n = 8$ per group). (e) Schematic timeline for the study of effects of monoclonal antibody against CE12 (mAb-CE12) in BALB/c mice. (f) Anti-CE12-specific antibody in response to mAb-CE12 injection in BALB/c mice (ELISA on serum samples, $n = 8$ per group). (g) Systolic BP in response to mAb-CE12 injection in BALB/c mice ($n = 8$ per group). * $P < .05$ versus normal IgG. (h) Heart rate of the BALB/c mice ($n = 8$ per group). (i) Schematic timeline for the study of effects of Q β -CE12 vaccination in BALB/c mice. (j) Anti-CE12-specific antibody in response to Q β -CE12 vaccination in BALB/c mice (ELISA on serum samples, $n = 8$ per group). (k) Systolic BP in response to Q β -CE12 vaccination in BALB/c mice ($n = 8$ per group). * $P < .05$ versus Ang II. (l) Heart rate of the BALB/c mice ($n = 8$ per group). Data are expressed as mean \pm SEM, analysed by two-way repeated measures ANOVA. Aml, amlodipine; VLP, virus-like particle

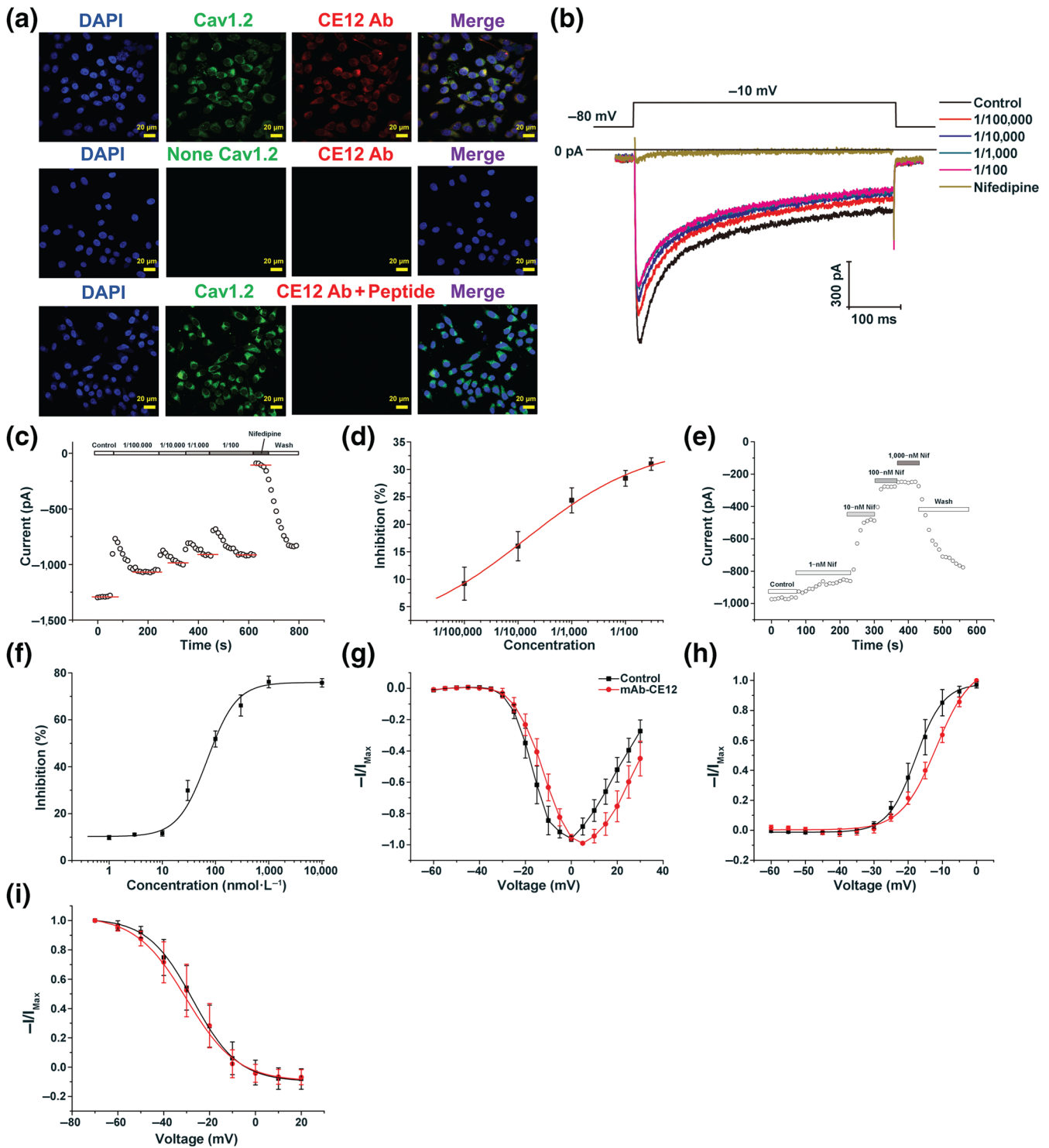


FIGURE 2 Monoclonal antibody against CE12 specifically binds to and inhibits the L-type calcium channel. (a) Specific binding of monoclonal antibody against CE12 (mAb-CE12) to $\text{Ca}_v1.2$ calcium channel. (b) Representative whole-cell $\text{Ca}_v1.2$ calcium currents in response to various concentrations of mAb-CE12 treatment. (c, d) Inhibition of $\text{Ca}_v1.2$ calcium currents by mAb-CE12 treatment ($n = 7$). (e, f) Inhibition of $\text{Ca}_v1.2$ calcium currents by nifedipine treatment ($n = 7$). (g) I-V relationship of $\text{Ca}_v1.2$ calcium channel after mAb-CE12 treatment ($n = 7$). (h) Activation curve of $\text{Ca}_v1.2$ calcium channel after mAb-CE12 treatment ($n = 7$). (i) Inactivation curve of $\text{Ca}_v1.2$ calcium channel after mAb-CE12 treatment ($n = 7$). Data are expressed as mean \pm SEM, analysed by two-way ANOVA. Cav1.2, $\text{Ca}_v1.2$ calcium channel; CE12 Ab, monoclonal antibody against CE12; Nif, nifedipine; None Cav1.2, not transfected with plasmid expressing $\text{Ca}_v1.2$ α_{1C} subunit; peptide, CE12 peptide

CE12-specific antibody was detected (Figure 1f). Prior to Ang II infusion, there is no difference in SBP levels among the groups. The SBP levels of mAb-CE12-injected mice were significantly lower than the normal mouse IgG group or the control group after Ang II infusion (Figure 1g). No significant differences in SBP levels were found between the control group and the normal mouse IgG group. The mice injected with 100 μ g of mAb-CE12 showed a greater decrease in SBP than the mice injected with 50 μ g of mAb-CE12. The heart rates of the mice among these groups were not statistically different (Figure 1h). Moreover, Q β -CE12 vaccine was tested in Ang II-induced hypertensive BALB/c mice (Figure 1i). Anti-CE12-specific antibody rose dramatically after the second Q β -CE12 vaccination and rose further after the third vaccination (Figure 1j). The SBP levels of the vaccine group and the amlodipine group were significantly decreased compared with the Ang II group, with a maximum decrease of 19 mmHg in the vaccine group (159 ± 2

vs. 178 ± 3 mmHg, Figure 1k). The heart rates of the mice were not significantly different (Figure 1l).

3.2 | Monoclonal antibody against CE12 specifically binds to and inhibits the L-type calcium channel

Immunofluorescence assays demonstrated that mAb-CE12 specifically bound to HEK293 cells stably expressing the human L-type Ca_v1.2 calcium channel α_{1C} subunit (Figure 2a). In HEK293 cells stably expressing Ca_v1.2 α_{1C} subunit, mAb-CE12 binding was observed (Figure 2a, first row). However, this binding was scarcely detectable in HEK293 cells not transfected with the plasmid expressing Ca_v1.2 α_{1C} subunit (Figure 2a, second row). No binding was observed when mAb-CE12 was neutralized by the CE12 peptide (Figure 2a, third

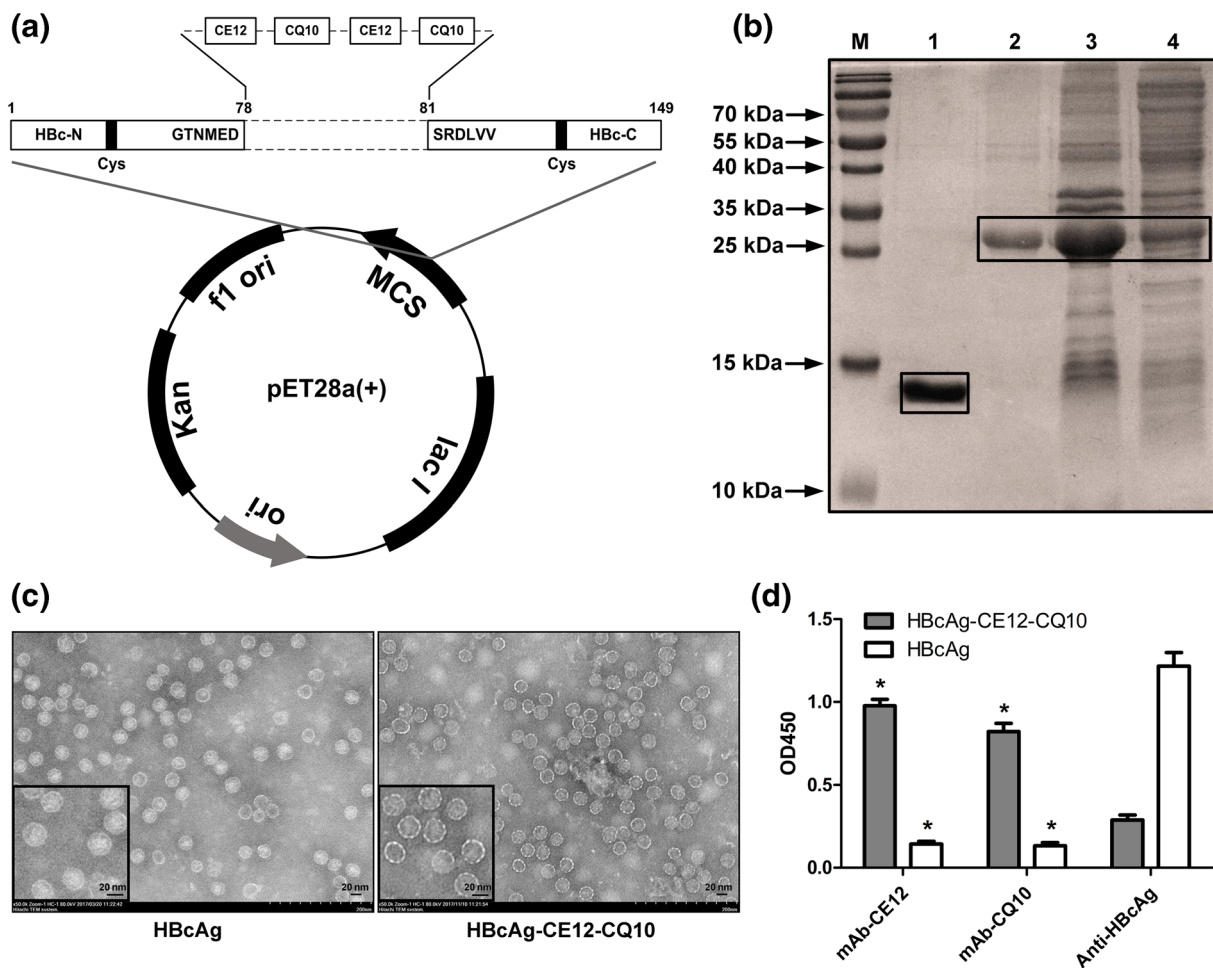


FIGURE 3 Construction and identification of the HBcAg-CE12-CQ10 vaccine. (a) Schematic map of the recombinant plasmid expressing the HBcAg-CE12-CQ10 protein. (b) SDS-PAGE analysis of the expression and purification products of the HBcAg-CE12-CQ10 protein. M, molecular marker; lane 1, renaturation product of the carboxyl-terminally truncated HBcAg (aa 1–149) protein; lane 2, renaturation product of the HBcAg-CE12-CQ10 protein; lane 3, precipitation of the expression lysate of bacteria transformed with plasmid expressing the HBcAg-CE12-CQ10 protein; lane 4, supernatant of the expression lysate of bacteria transformed with plasmid expressing the HBcAg-CE12-CQ10 protein. The boxes point out the recombinant proteins. (c) Transmission electron microscopy images of the purified virus-like particles. Smaller images in the bottom left corner indicate the representative images at higher magnification. (d) Specific binding of the epitopes by corresponding antibodies (n = 6). *P < .05 significantly different from anti-HBcAg. Data are expressed as mean \pm SEM, analysed by two-way ANOVA. HBcAg, carboxyl-terminally truncated HBcAg (aa 1–149) protein; mAb-CE12, monoclonal antibody against CE12; mAb-CQ10, monoclonal antibody against CQ10; OD450, OD at 450 nm

row). Next, we assessed the effects of mAb-CE12 on HEK293 cells that stably expressing the human L-type $\text{Ca}_v1.2$ calcium channel. Currents were evoked by a single 400-ms depolarizing pulse to -10 mV from the holding potential of -80 mV. Figure 2b shows the examples of whole-cell current traces before and after perfusion with 1/100,000, 1/10,000, 1/1,000, and 1/100 mAb-CE12 and nifedipine of $100 \mu\text{mol}\cdot\text{L}^{-1}$. Concentration-dependent inhibition of $\text{Ca}_v1.2$ current was observed with 1/100,000–1/100 mAb-CE12. Under the highest inhibition efficiency, about 30% of the maximum $\text{Ca}_v1.2$ calcium current was inhibited (Figure 2c,d). In comparison, nifedipine inhibited 80% of the maximum $\text{Ca}_v1.2$ calcium current (Figure 2e,f). As shown in Figure 2g, mAb-CE12 inhibited the calcium current with an obviously rightward shift of the I–V curve. It was found that mAb-CE12 could significantly shift the steady-state activation curve: $V_{1/2}$ values were -17.78 ± 0.59 mV of control and -11.80 ± 0.72 mV of 1:100 mAb-CE12 (Figure 2h). However, the mAb-CE12 ($10 \mu\text{g}\cdot\text{ml}^{-1}$) did not significantly shift the steady-state inactivation curve towards hyperpolarizing direction (Figure 2i). The $V_{1/2}$ $\text{Ca}_v1.2$ inactivation was -27.23 ± 0.64 mV in control and -30.14 ± 1.21 mV with mAb-CE12 ($10 \mu\text{g}\cdot\text{ml}^{-1}$).

3.3 | Construction and identification of the HBcAg-CE12-CQ10 vaccine

Carboxyl-terminally truncated HBcAg (aa 1–149) was used as an immune-enhancing carrier to present the selected epitopes. The gene sequences encoding the CE12 and CQ10 peptides were inserted into the DNA sequence encoding the MIR of HBcAg (Figure 3a). The resulting fusion protein was expressed in *E. coli* and purified thereafter. SDS-PAGE analysis validated the expression of the fusion protein (Figure 3b). To directly confirm the structure of the chimeric particles, the purified sample was subjected to negative-staining TEM. Empty particles with a diameter of about 30 nm were observed (Figure 3c). A discernible beaded string-like appearance of the capsid where foreign epitopes inserted in was observed at higher magnification (Figure 3c). To test the ability of the chimeric particles to present foreign epitopes, mAb-CE12, mAb-CQ10, or anti-HBcAg antibody (ab8639, Abcam) was co-incubated with ELISA plates coated with HBcAg or HBcAg-CE12-CQ10, respectively. The anti-HBcAg antibody specifically binds to amino acid positions 1–10 of HBcAg. The results revealed that the chimeric particle showed a predominant exposure of CE12 and CQ10 epitopes rather than the HBcAg epitopes (Figure 3d).

3.4 | HBcAg-CE12-CQ10 vaccination decreases BP of hypertensive rodents

To assess the effect of HBcAg-CE12-CQ10 vaccination on SBP, male SHR mice aged 4 weeks were injected subcutaneously on Days 0, 14, 28, 56, 84, and 98 with Q β -CQ10, Q β -CE12, or HBcAg-CE12-CQ10 vaccine, or PBS, respectively (Figure 4a). The SBP, anti-CE12-specific antibody, and anti-CQ10-specific antibody were examined periodically (Figure 4a). The titres of the anti-CE12-specific antibody (Figure 4b)

and anti-CQ10-specific antibody (Figure 4c) both showed a sharp rise after the second vaccination and rose further after the third vaccination and then declined gradually until the next vaccination. In comparison, HBcAg-CE12-CQ10 vaccination-induced antibody titres against CQ10 or CE12 were lower than those induced by Q β -CQ10 or Q β -CE12 throughout the study (Figure 4b,c). Moreover, in contrast to Q β -CQ10 or Q β -CE12, HBcAg-CE12-CQ10 vaccination may not induce dominant antibody against the carrier protein (Figure 4b,c). SBP levels of the Q β -CQ10, Q β -CE12, or HBcAg-CE12-CQ10 vaccinated groups and chemical drugs treated group were decreased compared with the SHRs received PBS (Figure 4d and Table 1). Compared with the control group, SBP levels of SHRs immunized with HBcAg-CE12-CQ10 vaccine showed a maximum decrease of 25 mmHg (150 ± 3 vs. 175 ± 2 mmHg, Table 1). The maximum SBP decrease was slightly less than that of chemical drugs, though no significant differences were observed between HBcAg-CE12-CQ10 vaccinated group and the group treated with chemical drugs. Notably, the HBcAg-CE12-CQ10 vaccinated group showed greater antihypertensive effects in comparison with the Q β -CQ10 or Q β -CE12 vaccinated group after the third and fourth immunization and later time points (Table 1). The heart rates of the SHRs among these groups were not statistically different (Figure 4e). Further, HBcAg-CE12-CQ10 vaccine was tested in Ang II-induced hypertensive mice (Figure 4f). Anti-CE12-specific and anti-CQ10-specific antibodies both rose markedly after the second immunization and rose further after the third immunization (Figure 4g). SBP levels of the vaccinated mice showed a steady decline compared with the Ang II group, with a maximum decrease of 35 mmHg (143 ± 3 vs. 178 ± 3 mmHg, Figure 4h). No significant difference of heart rate was found among the groups (Figure 4i).

3.5 | HBcAg-CE12-CQ10 vaccination ameliorates L-NAME-induced renal injury in SHRs

To induce severe renal injury, L-NAME was administered in drinking water to SHRs, for 4 weeks (Figure 4a). After the SHRs were killed, the kidneys were rapidly excised for pathological assessment. Examination of renal histology revealed that L-NAME treatment resulted in marked renal fibrosis (Figure 5a). Interstitial fibrosis was prominent in the cortical regions in the L-NAME group (Figure 5a). The extent of interstitial fibrosis was quantified by Masson trichrome staining. The percentage of fibrotic area was significantly reduced in the HBcAg-CE12-CQ10, Q β -CQ10, and the chemical drugs treated groups, but not in the Q β -CE12 group (Figure 5b). Obvious glomerular basement membrane thickening and diffuse foot process fusion was observed by TEM in the L-NAME group (Figure 5a). This pathological change was significantly attenuated in the HBcAg-CE12-CQ10, Q β -CQ10, and the chemical drugs treated groups (Figure 5c). After the administration of L-NAME, the levels of urine protein, blood urea nitrogen, and creatinine increased markedly in the L-NAME group. This increase was significantly attenuated in the HBcAg-CE12-CQ10, Q β -CQ10, and the chemical drugs treated groups, but not in the Q β -CE12 group (Figure 5d–f). Survival analysis indicated that the SHRs in the HBcAg-

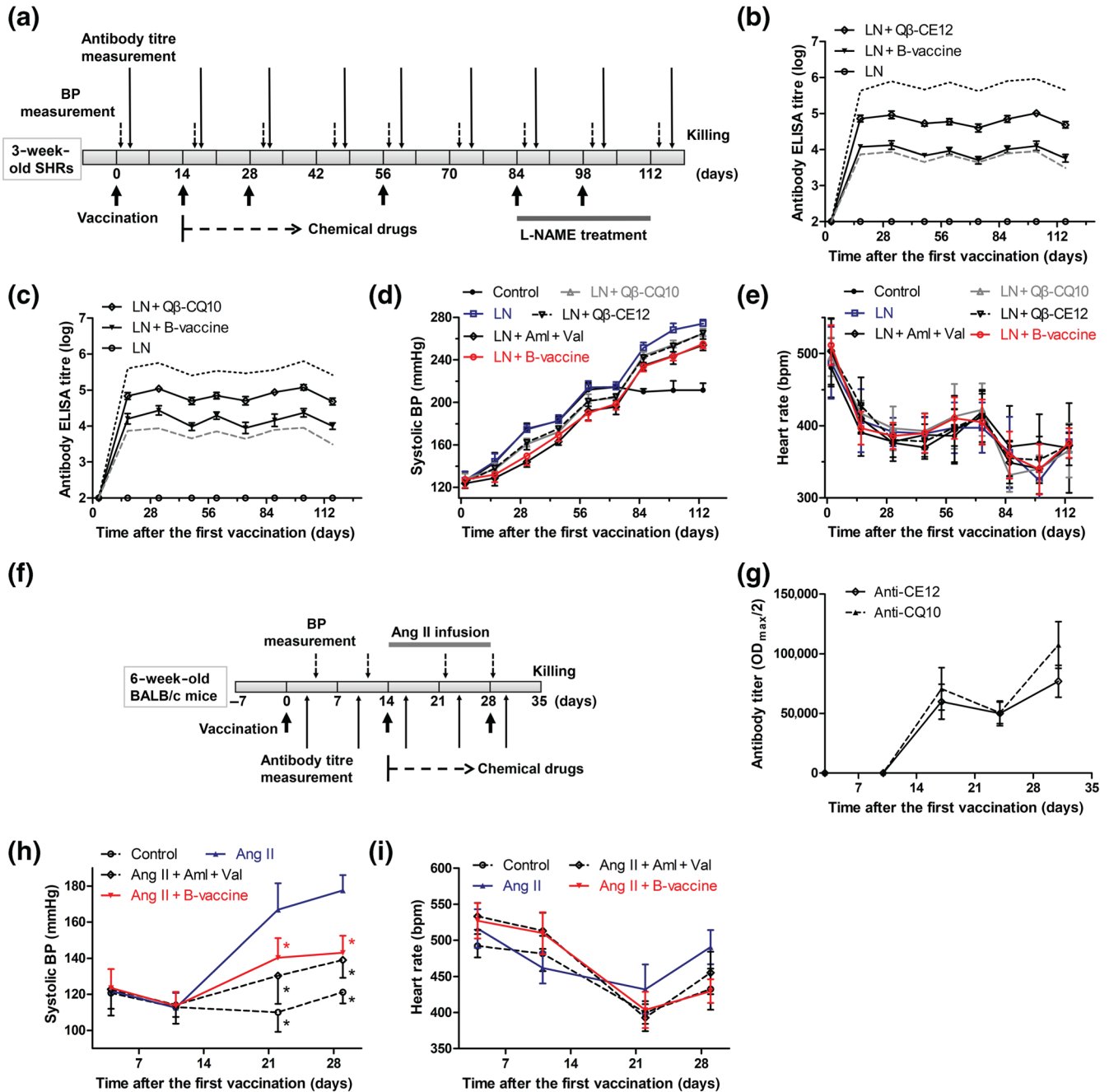


FIGURE 4 Antihypertensive effect of HBcAg-CE12-CQ10 vaccine in hypertensive rodents. (a) Schematic timeline for the study of effects of HBcAg-CE12-CQ10 vaccination in spontaneously hypertensive rats (SHRs). (b) Anti-CE12-specific antibody in response to immunization in SHRs (ELISA on serum samples, $n = 8$ per group). The black solid lines indicate antibodies against CE12, the black dotted line indicates antibody against Q β induced by Q β -CE12 vaccination, and the grey dashed line indicates antibody against HBcAg induced by HBcAg-CE12-CQ10 vaccination. (c) Anti-CQ10-specific antibody in response to immunization in SHRs (ELISA on serum samples, $n = 8$ per group). The black solid lines indicate antibodies against CQ10, the black dotted line indicates antibody against Q β induced by Q β -CQ10 vaccination, and the grey dashed line indicates antibody against HBcAg induced by HBcAg-CE12-CQ10 vaccination. (d) Systolic BP in response to immunization in SHRs ($n = 8$ per group). (e) Heart rate of the SHRs ($n = 8$ per group). (f) Schematic timeline for the study of effects of HBcAg-CE12-CQ10 vaccination in BALB/c mice. (g) Antibody titres in response to immunization in BALB/c mice (ELISA on serum samples, $n = 8$ per group). (h) Systolic BP in response to immunization in BALB/c mice ($n = 8$ per group). * $P < .05$ versus Ang II. (i) Heart rate of the BALB/c mice ($n = 8$ per group). Data are expressed as mean \pm SEM, analysed by two-way repeated measures ANOVA. Aml, amlodipine; B-vaccine, bivalent HBcAg-CE12-CQ10 vaccine; LN, L-NAME; Val, valsartan

TABLE 1 Antihypertensive effect of HBcAg-CE12-CQ10 vaccination in spontaneously hypertensive rats (mmHg)

Time (day)	Control (n = 8)	LN (n = 8)	LN + Q β -CQ10 (n = 8)	LN + Q β -CE12 (n = 8)	LN + Aml + Val (n = 8)	LN + B-vaccine (n = 8)
2	125 \pm 3	126 \pm 3	128 \pm 2	125 \pm 2	124 \pm 2	127 \pm 3
16	143 \pm 3	144 \pm 3	137 \pm 2	138 \pm 2	129 \pm 3 ^{*,δ}	132 \pm 3 ^{*,δ}
31	175 \pm 2	175 \pm 2	161 \pm 2 ^{*,δ,#}	162 \pm 2 ^{*,δ,#}	144 \pm 2 ^{*,δ}	150 \pm 3 ^{*,δ}
46	183 \pm 1	183 \pm 2	172 \pm 1 ^{*,δ}	175 \pm 1 ^{*,δ}	163 \pm 1 ^{*,δ}	169 \pm 2 ^{*,δ}
60	212 \pm 2	214 \pm 2	202 \pm 2 ^{*,δ,#}	201 \pm 2 ^{*,δ,#}	192 \pm 3 ^{*,δ}	190 \pm 3 ^{*,δ}
73	215 \pm 2	215 \pm 2	204 \pm 1 ^{*,δ}	205 \pm 1 ^{*,δ}	196 \pm 3 ^{*,δ}	199 \pm 2 ^{*,δ}
86	210 \pm 1*	251 \pm 2 ^{δ}	244 \pm 1 ^{*,δ,#}	242 \pm 2 ^{*,δ,#}	234 \pm 2 ^{*,δ}	234 \pm 2 ^{*,δ}
100	212 \pm 3*	268 \pm 2 ^{δ}	254 \pm 1 ^{*,δ,#}	253 \pm 2 ^{*,δ,#}	244 \pm 3 ^{*,δ}	243 \pm 1 ^{*,δ}
114	212 \pm 2*	274 \pm 2 ^{δ}	265 \pm 2 ^{*,δ,#}	265 \pm 2 ^{*,δ,#}	254 \pm 2 ^{*,δ}	255 \pm 1 ^{*,δ}

Note. All data are expressed as mean \pm SEM, analysed by two-way repeated measures ANOVA.

Abbreviations: Aml, amlodipine; B-vaccine, bivalent HBcAg-CE12-CQ10 vaccine; LN, L-NAME; Val, valsartan.

* $P < .05$, significantly different from LN; ^{δ} $P < .05$, significantly different from control. # $P < .05$, significantly different from LN + B-vaccine.

CE12-CQ10, Q β -CQ10, and the chemical drugs treated groups exhibited reduced mortality, compared with those in the L-NAME group, but this protective trend did not attain statistical significance (Figure 5g).

3.6 | No obvious immune-mediated injury and in vitro electrophysiological adverse effects are observed after HBcAg-CE12-CQ10 treatment

For safety consideration, histological changes in the heart, lung, liver, and kidney from the HBcAg-CE12-CQ10 immunized rats were examined by light microscopy and TEM. No evidence of skin damage at the site of subcutaneous injection was observed in vaccinated animals. No obvious tissue injury and inflammatory cells infiltration were observed in any of the organs (Figure 6a). TEM analysis of the kidney indicated that the structure of the basement membrane was intact and no immune complexes were observed in the vaccinated group (Figure 6b). Male BALB/c mice aged 7 weeks were immunized subcutaneously with 200 μ g of HBcAg-CE12-CQ10 vaccine on Days 0 and 14 to investigate T cell and B cell immune responses (Figure 6c). T helper (Th) cells differentiation diversity was not significant on Day 7 after the first vaccination, whereas after the second immunization, follicular helper T (Tfh) cells were up-regulated accompanied by a relative decline of Th1 cells (Figure 6d). As the most important Th cells to B cells, Tfh cells greatly promote B cell activation and antibody production. IgG antibodies are major effective antibodies. We observed a significant IgG1-dominant antibody production on Day 21, similar to most of the VLP-based vaccines (Figure 6e). On the other hand, levels of Th2 and Th17 cells were stable, indicating that the HBcAg-CE12-CQ10 vaccine may not induce a potent T cell-related autoimmune or inflammation damage. The long-QT syndrome is a major safety concern in the development and application of both cardiac and non-cardiac drugs. It is usually associated with pharmacological inhibition of cardiac hERG potassium channels (Kalyaanamoorthy & Barakat, 2018). To our satisfaction, no significant inhibitory effect of mAb-

CE12 on hERG current was recorded from HEK293 cells expressing hERG channels (Figure 6f). Also, Na_v1.5 sodium channels play an essential role in the initiation and propagation of the cardiac action potential. In our study, Na_v1.5 sodium current was not affected by mAb-CE12 (Figure 6g). As a result of L-NAME treatment, group sizes were unequal at the end of the study, and no significant alterations of the echocardiographic parameters of SHR were found (Table 2).

4 | DISCUSSION

In our present study, we designed an epitope derived from the L-type calcium channel and constructed the HBcAg-CE12-CQ10 vaccine that targeted both the AT₁ receptor and the L-type calcium channel. Our results showed that immunization with Q β -CE12 successfully reduced SBP in hypertensive rodents. In vitro studies found that monoclonal antibody against CE12 specifically bound to and inhibited the L-type calcium channel. Further, HBcAg-CE12-CQ10 vaccination decreased BP of hypertensive rodents and showed greater antihypertensive effects in comparison with the Q β -CQ10 or Q β -CE12 vaccination at certain time points. Besides, HBcAg-CE12-CQ10 vaccination ameliorated L-NAME-induced renal injury in SHR. No obvious immune-mediated injury or inhibitory effect on hERG current or Na_v1.5 current was observed. And HBcAg-CE12-CQ10 vaccination may not induce dominant antibodies against the carrier protein. Collectively, our study demonstrates that the HBcAg-CE12-CQ10 vaccine is basically safe and effective in the treatment of hypertension in rodent models.

VLPs are self-assembly systems characterized by highly repetitive and organized surface structures that can induce potent antibody responses (Bachmann & Jennings, 2010). Antigens displayed on VLPs assume a similar immunogenicity as the underlying particle (Bachmann & Jennings, 2010). However, in most cases, the epitopes conjugated with the carrier VLPs are not capable of blocking epitopes of the carrier protein effectively, and large numbers of the epitopes of the carrier protein are exposed to the lymphocytes which recognize them.

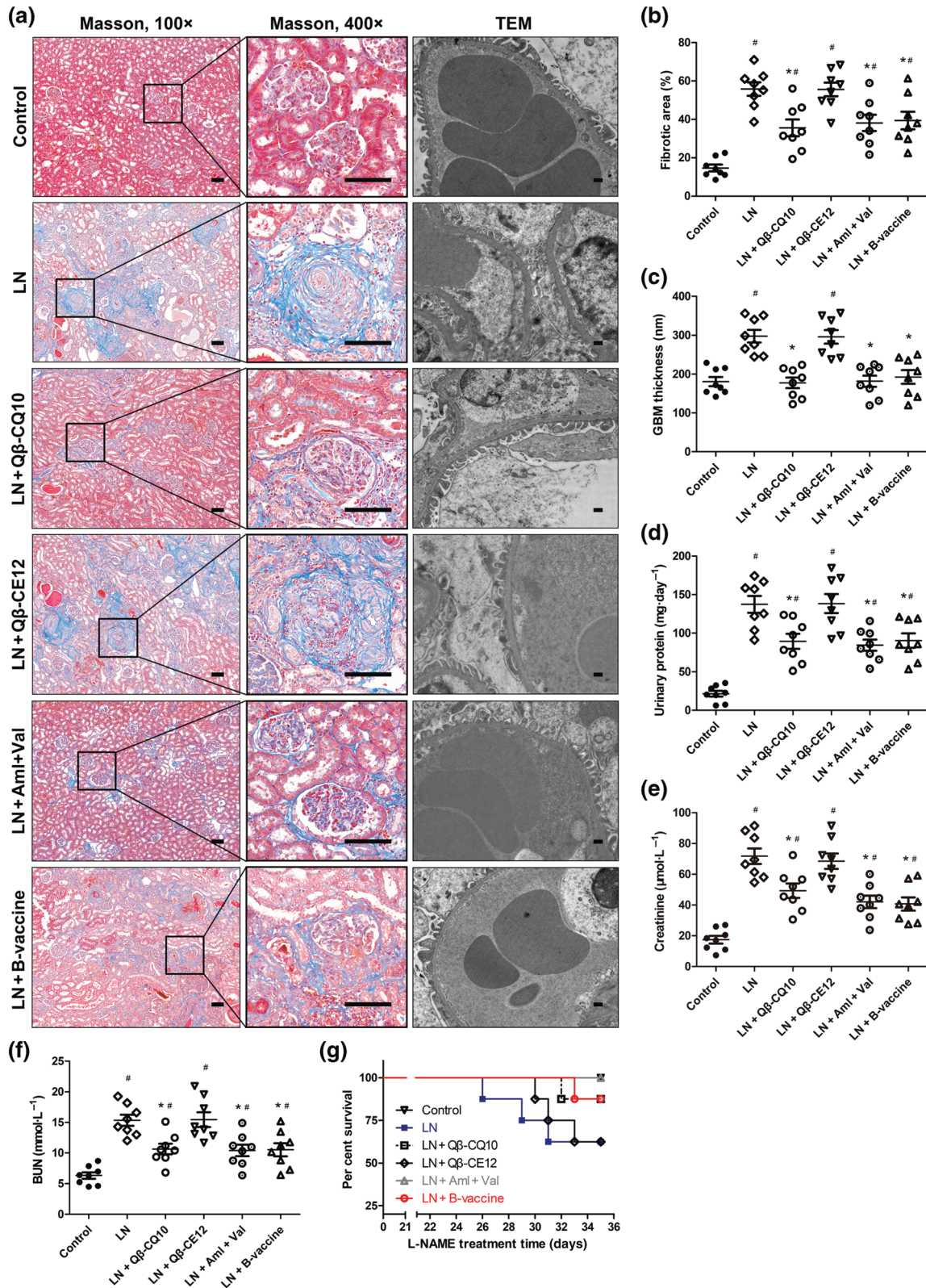


FIGURE 5 Renal protection effect of HBcAg-CE12-CQ10 vaccination in spontaneously hypertensive rats. (a) Representative images of Masson staining and transmission electron microscopy (TEM) of kidney. Bar in Masson images, 100 μm; bar in TEM images, 400 nm. (b) Quantitative analysis of renal fibrosis. (c) Quantitative analysis of glomerular basement membrane thickness. (d) Twenty-four hours of urinary protein. (e) Plasma creatinine level. (f) Blood urea nitrogen level. (g) Percentage of survival during L-NAME treatment. Data are expressed as mean ± SEM, analysed by one-way ANOVA. Survival analysis was performed with log-rank (Mantel-Cox) test. $n = 8$ per group. * $P < .05$, significantly different from LN, # $P < .05$, significantly different from control. Aml, amlodipine; B-vaccine, bivalent HBcAg-CE12-CQ10 vaccine; BUN, blood urea nitrogen; LN, L-NAME; Val, valsartan

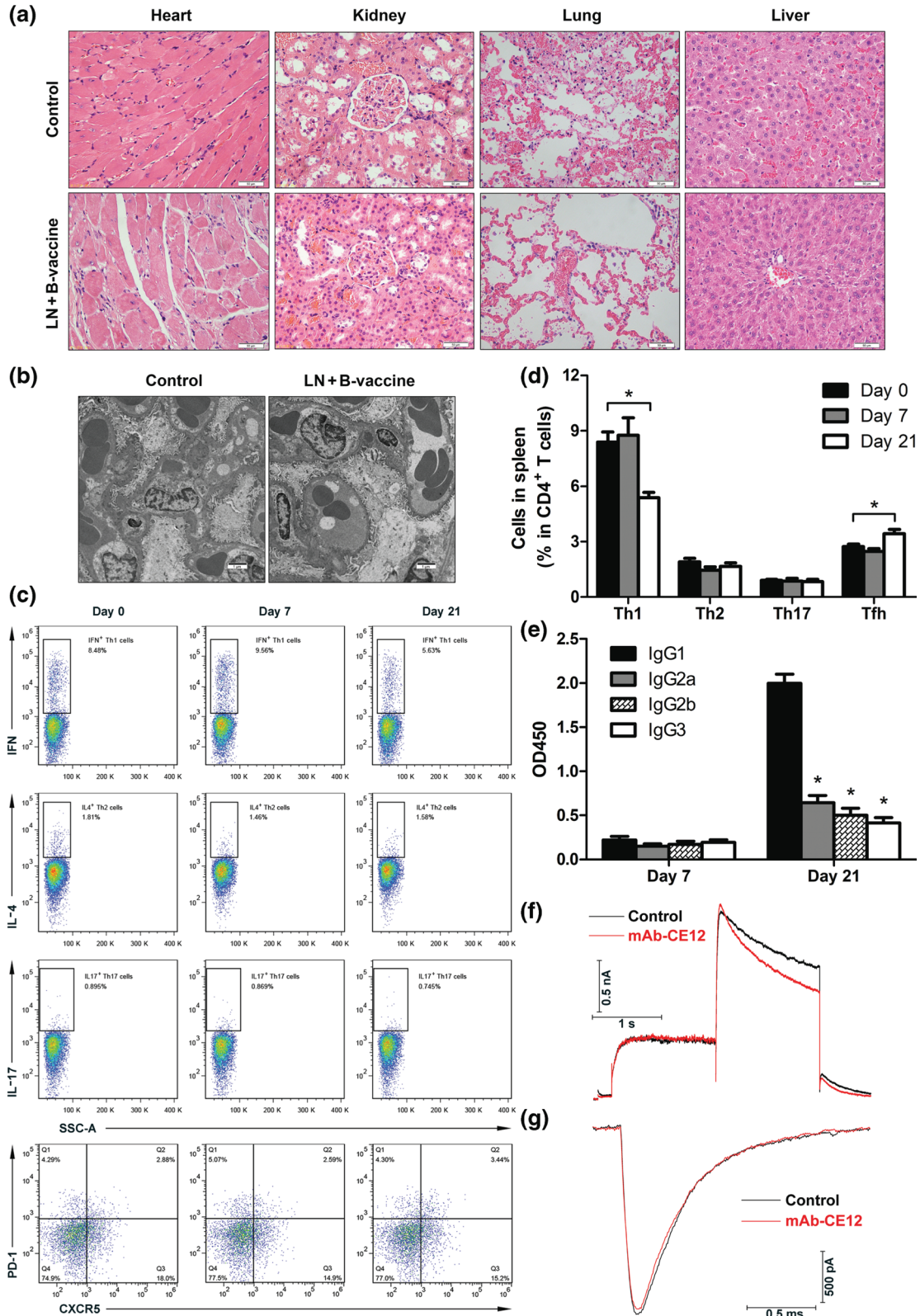


FIGURE 6 Safety assessment of the HBcAg-CE12-CQ10 vaccine. (a) Representative images of HE staining of heart, kidney, lung, and liver. (b) Representative TEM images of kidney. (c) Th1 (IFN- γ^+), Th2 (IL-4 $^+$), Th17 (IL-17 $^+$), and Tfh (CXCR5 $^+$) cells gated on CD4 $^+$ T cells. (d) Quantitative analysis of the percentages of Th1, Th2, Th17, and Tfh cells in CD4 $^+$ T cells ($n = 6$ per group). * $P < .05$, significantly different from Day 0 group. (e) IgG subclass after HBcAg-CE12-CQ10 vaccination in BALB/c mice ($n = 6$ per group). * $P < .05$, significantly different from IgG1. (f) Representative hERG current after mAb-CE12 treatment. (g) Representative Na $_v$ 1.5 sodium current after mAb-CE12 treatment. Data are expressed as mean \pm SEM, analysed by two-way ANOVA. B-vaccine, bivalent HBcAg-CE12-CQ10 vaccine; LN, L-NAME; OD450, OD at 450 nm; Tfh, follicular helper T cells.

TABLE 2 HBcAg-CE12-CQ10 vaccination had no effect on cardiac function

Parameter	Control (n = 8)	LN + Q β -CE12 (n = 5)	LN + B-vaccine (n = 7)
HR (bpm)	384.46 \pm 12.03	407.38 \pm 15.56	367.33 \pm 15.38
FS (%)	46.94 \pm 1.69	43.57 \pm 1.02	45.37 \pm 1.15
EF (%)	83.23 \pm 1.53	80.14 \pm 1.05	81.87 \pm 1.07
LVEDD (mm)	5.15 \pm 0.14	5.65 \pm 0.17	5.28 \pm 0.11
LVESD (mm)	2.33 \pm 0.07	2.51 \pm 0.07	2.42 \pm 0.06
LAESD (mm)	4.65 \pm 0.21	5.07 \pm 0.13	4.76 \pm 0.19
LAEDD (mm)	3.57 \pm 0.21	4.01 \pm 0.10	3.78 \pm 0.20
LVPWD (mm)	1.86 \pm 0.08	1.82 \pm 0.07	1.91 \pm 0.07
IVSD (mm)	1.77 \pm 0.05	1.89 \pm 0.08	1.90 \pm 0.05
LVAWD (mm)	1.89 \pm 0.08	2.00 \pm 0.11	1.99 \pm 0.06
LVPWS (mm)	2.71 \pm 0.07	2.69 \pm 0.09	2.83 \pm 0.07
IVSS (mm)	2.48 \pm 0.04	2.59 \pm 0.07	2.62 \pm 0.05
LVAWS (mm)	2.72 \pm 0.07	2.78 \pm 0.09	2.80 \pm 0.06

Note. All data are expressed as mean \pm SEM, analysed by one-way ANOVA.

Abbreviations: B-vaccine, bivalent HBcAg-CE12-CQ10 vaccine; EF, ejection fraction; FS, fractional shortening; HR, heart rate; IVSD, diastolic interventricular septum; IVSS, systolic interventricular septum; LAEDD, left atrial end-diastolic dimension; LAESD, left atrial end-systolic dimension; LN, L-NAME; LVAWD, diastolic left ventricular anterior wall; LVEDD, left ventricular end-diastolic dimension; LVESD, left ventricular end-systolic dimension; LVPWD, diastolic left ventricular posterior wall; LVPWS, systolic left ventricular posterior wall.

As a result, the conjugated vaccines induce dominant antibodies against the carrier protein instead of the conjugated peptide epitopes (Hu et al., 2017), which may impair the humoral immune response against the conjugated epitopes. HBcAg VLPs have been studied intensively and used as epitope carriers in previous clinical trials (Gregson et al., 2008; Nardin et al., 2004; Oliveira et al., 2005). The protruding spikes that locate within the MIR of HBcAg are considered the optimal targets for the display of foreign antigens (Pumpens & Grens, 2001). Tandem insertion of repeated foreign epitopes into the MIR of HBcAg led to increased steric hindrance for the exposure of carrier protein epitopes, and the dominant immune response against the carrier protein was greatly impaired (Roose et al., 2013). Besides, a previous study showed that antibodies against HBcAg have no effect on BP or hypertensive target organ damage (Koriyama et al., 2015). These evidences indicate that HBcAg VLPs might be advantageous tools for hypertension vaccine design.

DHPs are widely used in hypertension treatment by binding to the voltage-gated Ca_v1.2 calcium channel (Tang et al., 2016). The Ca²⁺ entering through the L-type calcium channel Ca_v1.2 serves as an essential intracellular messenger and regulates muscle contraction (Hofmann et al., 2014). In resistance vessels, the L-type calcium channel Ca_v1.2 is a key player in the hormonal regulation of BP and development of myogenic tone (Moosmang et al., 2003). Antibodies against voltage-gated calcium channels were detected in Lambert-Eaton

myasthenic syndrome patients and paraneoplastic cerebellar ataxia patients (Dalmau, Gultekin, & Posner, 1999; Liao et al., 2008). The antibodies were considered to have inhibited the P/Q-type and N-type calcium channels in presynaptic terminals (Liao et al., 2008). Increasing cases suggested the possibility of designing a vaccine targeting the L-type calcium channel Ca_v1.2 for the treatment of hypertension. A previous study revealed the importance of the E3 region for the function of ion channels (Xu et al., 2005). Antibodies against the potassium channel (Li et al., 2013), sodium channel (Korkmaz et al., 2013), and transient receptor potential channel (Lau et al., 2016) were successfully generated respectively under the guidance of this strategy. Based on the previous studies, the epitope CE12 was designed and examined. Electrophysiological analysis showed that mAb-CE12 inhibited 30% of the maximum Ca_v1.2 current under the highest inhibition efficiency. In our patch-clamp experiments, we found that mAb-CE12 was difficult to wash off once it bound to the Ca_v1.2 calcium channel (Figure 2c,e), which led to prolonged inhibition of the channel. Although further studies are needed to elucidate the mechanisms, this phenomenon may provide a reasonable explanation for the effective inhibition of Ca_v1.2 calcium channels by antibodies against CE12.

The L-type calcium channel Ca_v1.2 is expressed in various tissues including heart, smooth muscle, pancreas, adrenal gland, and brain (Hofmann et al., 2014). The extensive alternative splicing of the L-type calcium channel Ca_v1.2 leads to diverse splice variants with distinct electrophysiological and pharmacological properties (Liao, Yong, Liang, Yue, & Soong, 2005). The smooth muscle splice variant Ca_v1.2b is more sensitive to inhibition by DHPs than the heart variant Ca_v1.2a, because the former contains the DHP-sensitive exon 8B (Hofmann et al., 2014). This might be a possible explanation for the result that no obvious effect on heart beats was found after vaccination against L-type calcium channels. Nevertheless, further studies are needed to clarify the underlying reasons.

The titres of the antibodies against CE12 or CQ10 elicited by the bivalent vaccine were lower than those induced by Q β -CE12 or Q β -CQ10 vaccine, respectively, whereas the bivalent vaccine induced relatively superior antihypertensive effects compared with Q β -CE12 or Q β -CQ10 vaccine. In our view, the differences in the antibody titres may partly result from the difference in immunogenicity of VLP carriers. For another, Q β VLPs expressed in *E. coli* spontaneously package bacterial RNA during self-assembly process, and this RNA can act as a vaccine adjuvant as it triggers **toll-like receptor 8/9** in B cells (Foerster & Bachman, 2015). Moreover, the conjugated vaccines display the epitopes with only one end conjugated with the VLPs, while the other end wandering, which may result in diverse conformational changes and corresponding diversified antibodies. However, both N and C terminals of the antigen epitope in the natural target molecules are covalently bound with neighbouring amino acid residues in the target molecule, which greatly restricted the conformational change of the antigen epitope in natural target molecules. Therefore, probably a great deal of antibodies with lower affinity for the target molecule may be induced by conjugated vaccine immunization, and only part of or even small part of the antibodies induced by this immunization will fit the

natural epitope conformation perfectly. In contrast, both ends of the peptide inserted into the MIR of HBcAg were anchored, which may result in an unchanging structure and was similar to the native conformation of the epitope in target molecules. It is very likely that immunization with the bivalent HBcAg-CE12-CQ10 vaccine will induce homogenous antibodies with much higher affinity for the inserted epitopes. Consequently, antibodies against the antigen epitopes induced by the bivalent HBcAg-CE12-CQ10 vaccine may work with much higher efficiency compared with that induced by the conjugated vaccines. However, further studies are needed to test our speculations. Besides, combination drug therapy against multiple targets usually accomplishes greater antihypertensive effects in clinical practice when compared with the usage of a single drug. Thus, the combined effect of antibodies against CE12 and CQ10 induced by bivalent HBcAg-CE12-CQ10 vaccination would further strengthen the antihypertensive effects of the bivalent vaccine. It is noteworthy that the vaccinations did not reverse the BP or target organ injury to healthy levels. Further study is needed to achieve more efficient antihypertensive effect and target organ protection, and optimized adjuvant technologies that promote stronger immune responses or combination of vaccine with chemical drugs might be possible solutions.

In this study, the kidneys of the SHR_s administered with L-NAME were assessed as representatives of the vulnerable target organs of hypertension. NO is produced by the NOS and acts as an important regulator in vascular relaxation (Dinh, Drummond, Sobey, & Chrissobolis, 2014). Previous studies showed that the ROS are significantly increased in hypertensive animals (Dinh et al., 2014). The excessive ROS in hypertensive rats interact with NO and reduce NO bioavailability (Dinh et al., 2014). As an NOS inhibitor, L-NAME exacerbates this crisis and results in severe renal injury. In our previous work, the excessive production of ROS was inhibited by vaccination against AT₁ receptors, which may contribute to the target organ protection in hypertension (Ding et al., 2016; Zhou et al., 2016). In the present study, the renal protective effect was barely observed in SHR_s immunized with Q β -CE12. This discovery was roughly in line with a similar finding that DHPs are not so efficient in reversing severe oxidative stress associated with hypertension (El Hassar et al., 2015). Hence, the target organ protection effect in the bivalent vaccine group might be principally the contribution of specific antibodies against CQ10, but not CE12.

The safety of the HBcAg-CE12-CQ10 vaccine is an extremely important issue. A safety criterion of therapeutic vaccine involves four issues: the targeted molecule, reversible antibody response, antibody-dependent cell-mediated cytotoxicity, and induction of T cells against self-antigens (Bachmann & Dyer, 2004). Immune complex deposition is mostly observed in the kidney, especially in the glomerular basement membrane. In our study, immune complex deposition in the kidney was not detected by TEM. Besides, no visible pathological changes were observed by light microscopy in HBcAg-CE12-CQ10 vaccinated SHR_s. As for antibody-dependent cell-mediated cytotoxicity, the *in vivo* efficacy of this process is relatively ill defined, and it seems to be more of a theoretical concern than a practical problem (Bachmann & Dyer, 2004). Nevertheless, the potential effects caused by the vaccine needed further investigation. The antibody response

was reversible according to our observations, which indicated the possibility of halting antibody production. In our study, Th1 cells differentiation was significantly reduced after the second immunization, indicating that the activation of self-reactive T cells was avoided. Besides, HBcAg-CE12-CQ10 immunization enhanced Tfh cells differentiation after the second immunization. Tfh cells prime B cells to initiate antibody response and are crucial for maintenance of humoral immune memory (Vinuesa, Linterman, Yu, & MacLennan, 2016); our results indicate that HBcAg-CE12-CQ10 immunization induced a primarily Th2-type response and may not elicit an autoimmune response. Nevertheless, further studies will be necessary to determine whether autoimmune responses are induced by HBcAg-CE12-CQ10 vaccination.

Unintended blockade of hERG current remains a major impediment in delivering safe drugs to the clinic (Kalyaanamoorthy & Barakat, 2018). In our study, *in vitro* inhibition of hERG current was not observed. Na_v1.5 sodium channel plays an essential role in the initiation and propagation of the cardiac action potential. Our results showed that Na_v1.5 sodium channel was not affected by mAb-CE12. These findings might result from the diversity of E3 region between different ion channels (Xu et al., 2005) and suggest significantly reduced risks of cardiac arrhythmia induced by HBcAg-CE12-CQ10 immunization. From the results above, the HBcAg-CE12-CQ10 vaccine was found to be basically safe, although further assessments are needed to confirm this conclusion.

To our knowledge, this is the first time a vaccine targeting the L-type calcium channel was invented. Furthermore, the bivalent vaccine targeting both the AT₁ receptor and the L-type calcium channel was reported for the first time. We demonstrated that the bivalent vaccine targeting both the AT₁ receptor and the L-type calcium channel was basically safe and effectively reduced the BP in hypertensive rodent models and protected the target organ from hypertensive injury without obvious feedback activation of RAS and induction of dominant antibodies against the carrier protein, which may provide a novel strategy for hypertension vaccine design.

ACKNOWLEDGEMENTS

We thank Dr. Yimei Du at Research Center of Ion Channelopathy, Union Hospital, Tongji Medical College, Huazhong University of Science and Technology, for her invaluable help in revising the manuscript. This work was supported by the 7th "3551 China Optics Valley Talent Schema"; the Major Research Plan of the National Natural Science Foundation of China (91439207); and National Natural Science Foundation of China (81670461, 81600390, and 81500388).

AUTHOR CONTRIBUTIONS

X.C., Y.L., and A.Z. designed the experiments. H.W., Z.Q., and M.W. wrote the manuscript. H.W., Y.W., G.W., X.H., X.Y., and F.K. performed the experiments. Y.W. and H.Z. analysed the data.

CONFLICT OF INTEREST

The authors declare no conflict of interest.

DECLARATION OF TRANSPARENCY AND SCIENTIFIC RIGOUR

This declaration acknowledges that this paper adheres to the principles for transparent reporting and scientific rigour of preclinical research as stated in the *BJP* guidelines for [Design & Analysis](#), and [Animal Experimentation](#), and as recommended by funding agencies, publishers, and other organizations engaged with supporting research.

ORCID

Xiao Chen  <https://orcid.org/0000-0003-0294-4593>

REFERENCES

- Alexander, S. P. H., Christopoulos, A., Davenport, A. P., Kelly, E., Marrion, N. V., Peters, J. A., et al. (2017). The Concise Guide to PHARMACOLOGY 2017/18: G protein-coupled receptors. *British Journal of Pharmacology*, 1(174 Suppl), S17–S129.
- Alexander, S. P. H., Fabbro, D., Kelly, E., Marrion, N. V., Peters, J. A., Faccenda, E., ... CGTP Collaborators (2017a). The Concise Guide to PHARMACOLOGY 2017/18: Catalytic receptors. *British Journal of Pharmacology*, 174, S225–S271. <https://doi.org/10.1111/bph.13876>
- Alexander, S. P. H., Fabbro, D., Kelly, E., Marrion, N. V., Peters, J. A., Faccenda, E., ... CGTP Collaborators (2017b). The Concise Guide to PHARMACOLOGY 2017/18: Enzymes. *British Journal of Pharmacology*, 174, S272–S359. <https://doi.org/10.1111/bph.13877>
- Alexander, S. P. H., Striessnig, J., Kelly, E., Marrion, N. V., Peters, J. A., Faccenda, E., et al. (2017). The Concise Guide to PHARMACOLOGY 2017/18: Voltage-gated ion channels. *British Journal of Pharmacology*, 1(174 Suppl), S160–S194.
- Ambuhl, P. M., Tissot, A. C., Furlurija, A., Maurer, P., Nussberger, J., Sabat, R., et al. (2007). A vaccine for hypertension based on virus-like particles: Preclinical efficacy and phase I safety and immunogenicity. *Journal of Hypertension*, 25, 63–72.
- Bachmann, M., & Dyer, M. (2004). Therapeutic vaccination for chronic diseases: A new class of drugs in sight. *Nature Reviews. Drug Discovery*, 3, 81–88A.
- Bachmann, M. F., & Jennings, G. T. (2010). Vaccine delivery: A matter of size, geometry, kinetics and molecular patterns. *Nature Reviews. Immunology*, 10, 787–796.
- Chen, X., Qiu, Z., Yang, S., Ding, D., Chen, F., Zhou, Y., et al. (2013). Effectiveness and safety of a therapeutic vaccine against angiotensin II receptor type 1 in hypertensive animals. *Hypertension*, 61, 408–416.
- Curtis, M. J., Alexander, S., Cirino, G., Docherty, J. R., George, C. H., Giembycz, M. A., et al. (2018). Experimental design and analysis and their reporting II: Updated and simplified guidance for authors and peer reviewers. *British Journal of Pharmacology*, 175, 987–993.
- Dagan, R., Poolman, J., & Siegrist, C. A. (2010). Glycoconjugate vaccines and immune interference: A review. *Vaccine*, 28, 5513–5523.
- Dalmau, J., Gultekin, H., & Posner, J. (1999). Paraneoplastic neurologic syndromes: Pathogenesis and physiopathology. *Brain Pathology*, 9, 275–284.
- Ding, D., Du, Y., Qiu, Z., Yan, S., Chen, F., Wang, M., et al. (2016). Vaccination against type 1 angiotensin receptor prevents streptozotocin-induced diabetic nephropathy. *Journal of Molecular Medicine*, 94, 207–218.
- Dinh, Q. N., Drummond, G. R., Sobey, C. G., & Chrissobolis, S. (2014). Roles of inflammation, oxidative stress, and vascular dysfunction in hypertension. *BioMed Research International*, 2014, 406960.
- El Hassar, C., Merzouk, H., Merzouk, S. A., Malti, N., Meziane, A., & Narce, M. (2015). Long-term use of angiotensin II receptor antagonists and calcium-channel antagonists in Algerian hypertensive patients: Effects on metabolic and oxidative parameters. *Free Radical Biology & Medicine*, 79, 147–153.
- Foerster, J., & Bachman, M. (2015). Beyond passive immunization: Toward a nanoparticle-based IL-17 vaccine as first in class of future immune treatments. *Nanomedicine (London, England)*, 10, 1361–1369.
- Fogari, R., Zoppi, A., Mugellini, A., Maffioli, P., Lazzari, P., & Derosa, G. (2011). Role of angiotensin II in plasma PAI-1 changes induced by imidapril or candesartan in hypertensive patients with metabolic syndrome. *Hypertension Research: Official Journal of the Japanese Society of Hypertension*, 34, 1321–1326.
- Global Burden of Metabolic Risk Factors for Chronic Diseases Collaboration (2014). Cardiovascular disease, chronic kidney disease, and diabetes mortality burden of cardiometabolic risk factors from 1980 to 2010: A comparative risk assessment. *The Lancet Diabetes and Endocrinology*, 2, 634–647.
- Gregson, A. L., Oliveira, G., Othoro, C., Calvo-Calle, J. M., Thorton, G. B., Nardin, E., et al. (2008). Phase I trial of an alhydrogel adjuvanted hepatitis B core virus-like particle containing epitopes of Plasmodium falciparum circumsporozoite protein. *PLoS ONE*, 3, e1556.
- Harding, S. D., Sharman, J. L., Faccenda, E., Southan, C., Pawson, A. J., Ireland, S., et al. (2018). The IUPHAR/BPS Guide to PHARMACOLOGY in 2018: Updates and expansion to encompass the new guide to IMMUNOPHARMACOLOGY. *Nucleic Acids Research*, 46, D1091–D1106.
- Hofmann, F., Flockerzi, V., Kahl, S., & Wegener, J. W. (2014). L-type CaV1.2 calcium channels: From in vitro findings to in vivo function. *Physiological Reviews*, 94, 303–326.
- Hu, X., Deng, Y., Chen, X., Zhou, Y., Zhang, H., Wu, H., et al. (2017). Immune response of a novel ATR-AP205-001 conjugate anti-hypertensive vaccine. *Scientific Reports*, 7, 12580.
- Insel, R. A. (1995). Potential alterations in immunogenicity by combining or simultaneously administering vaccine components. *Annals of the New York Academy of Sciences*, 754, 35–47.
- Jegerlehner, A., Wiesel, M., Dietmeier, K., Zabel, F., Gatto, D., Saudan, P., et al. (2010). Carrier induced epitopic suppression of antibody responses induced by virus-like particles is a dynamic phenomenon caused by carrier-specific antibodies. *Vaccine*, 28, 5503–5512.
- Kalyaanamoorthy, S., & Barakat, K. H. (2018). Development of safe drugs: The hERG challenge. *Medicinal Research Reviews*, 38, 525–555.
- Karpas, A., Dremucheva, A., & Czepulkowski, B. (2001). A human myeloma cell line suitable for the generation of human monoclonal antibodies. *Proceedings of the National Academy of Sciences of the United States of America*, 98, 1799–1804.
- Kilkenny, C., Browne, W., Cuthill, I. C., Emerson, M., Altman, D. G., & Group NCRREGW (2010). Animal research: Reporting in vivo experiments: The ARRIVE guidelines. *British Journal of Pharmacology*, 160, 1577–1579.
- Koriyama, H., Nakagami, H., Nakagami, F., Osako, M. K., Kyutoku, M., Shimamura, M., et al. (2015). Long-term reduction of high blood pressure by angiotensin II DNA vaccine in spontaneously hypertensive rats. *Hypertension*, 66, 167–174.
- Korkmaz, S., Zitron, E., Bangert, A., Seyler, C., Li, S., Hegedus, P., et al. (2013). Provocation of an autoimmune response to cardiac voltage-gated sodium channel NaV1.5 induces cardiac conduction defects in rats. *Journal of the American College of Cardiology*, 62, 340–349.
- Lau, O. C., Shen, B., Wong, C. O., Tjong, Y. W., Lo, C. Y., Wang, H. C., et al. (2016). TRPC5 channels participate in pressure-sensing in aortic baroreceptors. *Nature Communications*, 7, 11947.

- Leong, X.-F., Ng, C.-Y., & Jaarin, K. (2015). Animal models in cardiovascular research: Hypertension and atherosclerosis. *BioMed Research International*, 2015, 528757.
- Li, J., Seyler, C., Wiedmann, F., Schmidt, C., Schweizer, P. A., Becker, R., et al. (2013). Anti-KCNQ1 K(+) channel autoantibodies increase IKs current and are associated with QT interval shortening in dilated cardiomyopathy. *Cardiovascular Research*, 98, 496–503.
- Liao, J., Zhang, Y., Ye, F., Zhang, L., Chen, Y., Zeng, F., et al. (2016). Epigenetic regulation of L-type voltage-gated Ca²⁺ channels in mesenteric arteries of aging hypertensive rats. *Hypertension Research*, 40, 441–449.
- Liao, P., Yong, T. F., Liang, M. C., Yue, D. T., & Soong, T. W. (2005). Splicing for alternative structures of Cav1.2 Ca²⁺ channels in cardiac and smooth muscles. *Cardiovascular Research*, 68, 197–203.
- Liao, Y. J., Safa, P., Chen, Y.-R., Sobel, R. A., Boyden, E. S., & Tsien, R. W. (2008). Anti-Ca²⁺ channel antibody attenuates Ca²⁺ currents and mimics cerebellar ataxia in vivo. *Proceedings of the National Academy of Sciences of the United States of America*, 105, 2705–2710.
- Lobo, M. D., Sobotka, P. A., & Pathak, A. (2017). Interventional procedures and future drug therapy for hypertension. *European Heart Journal*, 38, 1101–1111.
- Lu, Y., Chan, W., Ko, B. Y., VanLang, C. C., & Swartz, J. R. (2015). Assessing sequence plasticity of a virus-like nanoparticle by evolution toward a versatile scaffold for vaccines and drug delivery. *Proceedings of the National Academy of Sciences of the United States of America*, 112, 12360–12365.
- Mancia, G., Fagard, R., Narkiewicz, K., Redon, J., Zanchetti, A., Bohm, M., et al. (2013). 2013 ESH/ESC guidelines for the management of arterial hypertension: The Task Force for the Management of Arterial Hypertension of the European Society of Hypertension (ESH) and of the European Society of Cardiology (ESC). *European Heart Journal*, 34, 2159–2219.
- McGrath, J. C., & Lilley, E. (2015). Implementing guidelines on reporting research using animals (ARRIVE etc.): New requirements for publication in BJP. *British Journal of Pharmacology*, 172, 3189–3193.
- Mills, K. T., Bundy, J. D., Kelly, T. N., Reed, J. E., Kearney, P. M., Reynolds, K., et al. (2016). Global disparities of hypertension prevalence and control: A systematic analysis of population-based studies from 90 countries. *Circulation*, 134, 441–450.
- Moosmang, S., Schulla, V., Welling, A., Feil, R., Feil, S., Wegener, J., et al. (2003). Dominant role of smooth muscle L-type calcium channel Ca_v1.2 for blood pressure regulation. *The EMBO Journal*, 22, 6027–6034.
- Nardin, E. H., Oliveira, G. A., Calvo-Calle, J. M., Wetzel, K., Maier, C., Birkett, A. J., et al. (2004). Phase I testing of a malaria vaccine composed of hepatitis B virus core particles expressing Plasmodium falciparum circumsporozoite epitopes. *Infection and Immunity*, 72, 6519–6527.
- NCD Risk Factor Collaboration (2017). Worldwide trends in blood pressure from 1975 to 2015: A pooled analysis of 1479 population-based measurement studies with 19.1 million participants. *Lancet*, 389, 37–55.
- Ngiow, S. F., Loi, S., Thomas, D., & Smyth, M. J. (2016). Mouse models of tumor immunotherapy. *Advances in Immunology*, 130, 1–24.
- Oliveira, G. A., Wetzel, K., Calvo-Calle, J. M., Nussenzweig, R., Schmidt, A., Birkett, A., et al. (2005). Safety and enhanced immunogenicity of a hepatitis B core particle Plasmodium falciparum malaria vaccine formulated in adjuvant Montanide ISA 720 in a phase I trial. *Infection and Immunity*, 73, 3587–3597.
- Oparil, S., & Schmieder, R. E. (2015). New approaches in the treatment of hypertension. *Circulation Research*, 116, 1074–1095.
- Pumpens, P., & Grens, E. (2001). HBV core particles as a carrier for B cell/T cell epitopes. *Intervirology*, 44, 98–114.
- Roose, K., De Baets, S., Schepens, B., & Saelens, X. (2013). Hepatitis B core-based virus-like particles to present heterologous epitopes. *Expert Review of Vaccines*, 12, 183–198.
- Tang, L., Gamal El-Din, T. M., Swanson, T. M., Pryde, D. C., Scheuer, T., Zheng, N., et al. (2016). Structural basis for inhibition of a voltage-gated Ca²⁺ channel by Ca²⁺ antagonist drugs. *Nature*, 537, 117–121.
- Tissot, A. C., Maurer, P., Nussberger, J., Sabat, R., Pfister, T., Ignatenko, S., et al. (2008). Effect of immunisation against angiotensin II with CYT006-AngQb on ambulatory blood pressure: A double-blind, randomised, placebo-controlled phase IIa study. *Lancet*, 371, 821–827.
- Vinuesa, C. G., Linterman, M. A., Yu, D., & MacLennan, I. C. (2016). Follicular helper T cells. *Annual Review of Immunology*, 34, 335–368.
- Wald, D. S., Law, M., Morris, J. K., Bestwick, J. P., & Wald, N. J. (2009). Combination therapy versus monotherapy in reducing blood pressure: Meta-analysis on 11,000 participants from 42 trials. *The American Journal of Medicine*, 122, 290–300.
- Whelton, P. K., Carey, R. M., Aronow, W. S., Casey, D. E. Jr., Collins, K. J., Dennison Himmelfarb, C., et al. (2018). 2017 ACC/AHA/AAPA/ABC/ACPM/AGS/APhA/ASH/ASPC/NMA/PCNA guideline for the prevention, detection, evaluation, and management of high blood pressure in adults: Executive summary: A report of the American College of Cardiology/American Heart Association Task Force on Clinical Practice Guidelines. *Hypertension*, 71, 1269–1324.
- Xu, S. Z., Zeng, F., Lei, M., Li, J., Gao, B., Xiong, C., et al. (2005). Generation of functional ion-channel tools by E3 targeting. *Nature Biotechnology*, 23, 1289–1293.
- Zamponi, G. W., Striessnig, J., Koschak, A., & Dolphin, A. C. (2015). The physiology, pathology, and pharmacology of voltage-gated calcium channels and their future therapeutic potential. *Pharmacological Reviews*, 67, 821–870.
- Zhou, Y., Wang, S., Qiu, Z., Song, X., Pan, Y., Hu, X., et al. (2016). ATRQβ-001 vaccine prevents atherosclerosis in apolipoprotein E-null mice. *Journal of Hypertension*, 34, 474–485.
- Zhu, F., Liao, Y., Li, L., Cheng, M., Wei, F., Wei, Y., et al. (2006). Target organ protection from a novel angiotensin II receptor (AT₁) vaccine ATR12181 in spontaneously hypertensive rats. *Cellular & Molecular Immunology*, 3, 107–114.

SUPPORTING INFORMATION

Additional supporting information may be found online in the Supporting Information section at the end of the article.

How to cite this article: Wu H, Wang Y, Wang G, et al. A bivalent antihypertensive vaccine targeting L-type calcium channels and angiotensin AT₁ receptors. *Br J Pharmacol*. 2020;177:402–419. <https://doi.org/10.1111/bph.14875>